AFGL-TR-76-0049

RESEARCH IN SEISMOLOGY

Avi Ben-Menahem

The Weizmann Institute of Science
Department of Applied Mathematics
Rehovot, Israel

1 March 1976

Final Report
1 April 1973 - 31 March 1975

Approved for public release; distribution unlimited.

Sponsored by Advanced Research Projects Agency
ARPA Order No. 1795

AIR FORCE GEOPHYSICS LABORATORY
AIR FORCE SYSTEMS COMMAND
UNITED STATES AIR FORCE
HANSCOM AFB, MASSACHUSETTS 01731

Unclassified

SECURITY CLASSIFICATION OF THIS PAGE (When Data Entered)

REPORT DOCUMENTATION PAGE	READ INSTRUCTIONS BEFORE COMPLETING FORM
1. REPORT NUMBER: AFGL-TR-76-0049	2. GOVT ACCESSION NO. / 3. RECIPIENT'S CATALOG NUMBER
4. TITLE (and Subtitle): RESEARCH IN SEISMOLOGY.	5. TYPE OF REPORT & PERIOD COVERED: Final Report. 1 Apr 73-31 Mar 75
	6. PERFORMING ORG. REPORT NUMBER
7. AUTHOR(s): Ari Ben-Menahem	8. CONTRACT OR GRANT NUMBER(s): AFAFOSR-73-2528-73
9. PERFORMING ORGANIZATION NAME AND ADDRESS: The Weizmann Institute of Science, Department of Applied Mathematics, Rehovot, (Israel),	10. PROGRAM ELEMENT, PROJECT, TASK, AREA & WORK UNIT NUMBERS: ARPA Order [illegible]-1795
11. CONTROLLING OFFICE NAME AND ADDRESS: Air Force Geophysics Laboratory(LW), Hanscom AFB, Massachusetts 01731, Monitor: Ker C. Thomson, LW	12. REPORT DATE: 1 Mar 1976
	13. NUMBER OF PAGES: 89
14. MONITORING AGENCY NAME & ADDRESS(if different from Controlling Office) 91p.	15. SECURITY CLASS. (of this report): Unclassified
	15a. DECLASSIFICATION/DOWNGRADING SCHEDULE

16. DISTRIBUTION STATEMENT (of this Report)

Approved for public release; distribution unlimited.

17. DISTRIBUTION STATEMENT (of the abstract entered in Block 20, if different from Report)

18. SUPPLEMENTARY NOTES

Sponsored by Advanced Research Projects Agency
ARPA Order No. 1795

19. KEY WORDS (Continue on reverse side if necessary and identify by block number)

Seismology, earthquakes, tectonics, crustal structure, seismicity, earth models, elastic wave motion

20. ABSTRACT (Continue on reverse side if necessary and identify by block number)

Research in seismology during the period April 1973 to March 1975 was concerned with the mechanisms and focal processes of Asian earthquakes, meteor impacts, and explosions. The seismicity, tectonics, and structure of the Afro-Eurasian junction, a complex region of relatively low seismic activity was clarified in terms of the breaking of an incoheretn plate. Theoretical seismograms for real earth and source models were applied to earthquake dislocation sources and to low-magnitude earthquakes and crustal structure analyses in

DD FORM 1 JAN 73 1473 EDITION OF 1 NOV 65 IS OBSOLETE

SECURITY CLASSIFICATION OF THIS PAGE (When Data Entered)

400 763

the northern Red Sea region. Generalized ray theory and reflection and transmission coefficients were applied to surface and shallow seismic sources in multi layered spherical earth models. Elastic wave motion processes across vertical discontinuities were studied.

Table of Contents

(1) Focal Processes of Earthquakes, Meteor Impacts and Atmospheric Nuclear Explosions. (Ben-Menahem, Vered, Aboodi and Schild)

All known tools of modern seismology were used to interpret observed seismograms from the following five events:

(a) The great Assam earthquake of Aug. 15, 1950.

(b) The Siberian atmospheric explosion of June 30, 1908.

(c) The Chinese atmospheric nuclear explosions of June 17, 1967 and Oct. 14, 1970.

(d) The Soviet atmospheric explosion of Oct. 30, 1961.

(a) The Assam earthquake

The source of the Assam earthquake of Aug. 15, 1950 is revealed from amplitude observations of surface and body waves at Pasadena, Tokyo and Bergen. Seiches' amplitudes in Norway, initial P motions throughout the world, aftershocks and landslides distribution, PP/P ratio at Tokyo, R/L ratio and directivity at Pasadena, are also used. The ensuing fault geometry and kinematics is consistent with the phenomenology of the event and the known geology of the source area. It is found that a progressive strike-slip rupture with velocity 3 km/sec took place on a fault of length 250 km with width 80 km striking 330-337° east of north and dipping 55-60° to ENE. The use of exact surface-wave theory and asymptotic body-wave theory with takes into account finiteness and absorption, rendered an average shear dislocation of 25 m. A three-dimensional theory for the excitation of seiches in lakes by the horizontal acceleration of surface waves was developed. It is confirmed that Love waves near Bergen generated seiches with peak amplitude up to 70 cm depending strongly on the width of the channel.

It is believed that the earthquake was caused by a motion of the Asian plate relative to the eastern flank of the Indian plate where the NE Assam

block is imparted a tendency of rotation with fracture lines being developed along its periphery.

Comparison with other well-studied earthquakes shows that although the magnitude of the Assam event superseded that of all earthquakes since 1950, its potency $U_o dS$ (700,000 m x km^2) was inferior to that of Alaska 1964 (1,560,000 m x km^2) and Chile 1960 (1,020,000 m x km^2).

An earthquake, which may perhaps be considered as one of the most devastating shocks ever recorded, struck the province of Assam, in northeast India, on Aug. 15, 1950 at about 14 09 30 G.C.T. The epicenter of this shock was found to be somewhat to the northeast of the major seismic zone of Assam and is just where the NNE-SW Burma structural axes meet the east-west structural lines of the Hsmalayas. It is one of the few earthquakes to which the instrumentally determined magnitude 8.6-8.7, was assigned. It was felt over an estimated area of 3 million km^2 in India, Burma, East Pakistan, Tibet and China and caused some 1500 deaths. The earthquake has severe effects on topography and the regime of rivers: Riverbeds had considerably silted up and many had permanently changed their courses, adding the effects of floods to those of shaking. Aerial reconnaissance revealed that 10,000 km^2 of hill area were affected by landslides. The spread of aftershocks activity extended from about 91° to 97°E and 24° to 33°N with the epicenter of the main shock near the eastern margin. Damage to roads, railways, bridges and buldings was extensive and the estimated acceleration on alluvium in the epicentral region was 0.5 g. A vivid description of the event was given by an eye-witness in the village of Rima, some 40 km east of the epicenter:

"Suddenly, after the faintest tremor there came an appalling noise and the earth began to shudder violently...I have a distinct recollection of seeing the outlines of the landscape, visible against the starry sky, blurred -

every ridge and tree fuzzy - as though it were rapidly moving up and down... We were immediately thrown to the ground...I find it very difficult to recollect my emotions during the four or five minutes the shock lasted, but the first feeling of bewilderment - an incredulous astonishment that these solid-looking hills were in the grip of a force which shook them as a terrier shakes a rat - gave place to stark terror ...

"The earthquake was now full under way, and it felt as though a powerful ram were hitting against the earth beneath us with the persistance of a kettledrum... The din was terrible, but it was difficult to separate the noise made by the earthquake itself from the roar of the rock avalanches pouring down on all sides into the basin...

"Day after day, night after night, tremors followed each other. Many of them were severe, and were always preceded by a short roar, like a distant thunder clap..."

Short-period seismographs all over the world recorded the earthquake. Long-period recordings were restricted to Benioff's strainmeter and a 1-90 seismograph system at Pasadena, a Press-Ewing seismograph at Lamont, an other 1-90 at Weston and an Omori seismograph at Tokyo. Actual ground motions due to crustal Love and/or Rayleigh waves at TOK, BER, STU, KEW and STR reached the level of the order of 10 mm and the Airy phase ground motion of R_3 at Pasadena measured two full millimeters. Seismic seiches in Norway and England, caused by the shaking of lakes and fjords by Love waves in the period range 60-180 sec, resulted in water-wave amplitudes up to 100 cm.

Macroseismic effects of the Assam earthquake were compiled, dispersion curves of surface waves at Japan were obtained and some recordings made by the Omori, Gray-Ewing and Hagiwara seismographs at Tokyo and Tukuba were presented. Long-period wave-forms, mostly multiple arrivals to Pasadena

and Lamont, were used to derive attenuation coefficients and Q-values for mantle surface waves.

The Assam earthquake has two interesting aspects: the mechanism by which the strain energy was released and the tectonic interpretation. While it is well accepted that the earthquakes of the greater Indian peninsula are the outcome of the Indian underthrust towards Asia, the behaviour at this particular region of Assam, which is a northeast wedge-like extension towards China, is unknown. Gansser dealt with the Assam region up to the Mishmi Hills southwest of the epicenter. The latter he described as a steep crystalline thrust running from SSE to NNW and either continuing into the main crystalline thrust of the Himalayas or into eastern Tibet. Evans considered Assam to be overthrusted from three sides: the eastern Himalayas from the north, the Naga Hills from the southeast, and the region SW to the epicenter from the northeast. Dutta considered the region as a special zone of seismic activity with block tectonics. The reaction of this zone was considered by him to be complicated because of the influence associated with both the Himalayas and Burmese force systems. As a whole he suggested that the NE Assam block is imparted a tendency of rotation with fracture lines being developed mainly along its periphery.

Focal-mechanism studies for the region did not tackle this major earthquake and concerned themselves mainly with events confirming the tectonic description of the Himalaya and Burma thrusts. Tandon solved the mechanism as a normal fault striking EW or between EW and NE-SW. He used initial-motion data from records and station bulletins. Some of the stations indicated as dilatational in his paper, reported as compressional to the ISS (New Delhi, Poona, Helwan). In fact, Poona seismograms indicate a compressional initial motion of P. Wickens and Hodgson used Tandon's data to find a thrust

mechanism with two planes dipping to the south and to the east, respectively.

In this report we aim at the interpretation of the Assam event in terms of the ambient tectonic forces. Every available piece of information known to us was considered.

Source parameters of the Assam earthquake of Aug. 15, 1950

Parameter	Symbol	Value
Fault length	b	250 km
Rupture velocity	v	3.0 km/sec
Width of fault	w	80 km
Depth of maximal dislocation	h	40--50 km
Vertical extent	H	65 km (~ crustal thickness)
Average dislocation	$\langle U_0(h)\rangle$	~35 m
Average potency	$\langle P\rangle = bw\langle U_0(h)\rangle$	700,000 m × km^2
Specific amplitude	$\Omega = \frac{U_0 dS}{4\pi a^2}$	1400 microns
Magnitude	M_S	8.6–8.7 (Richter, Brune)
Displacement time-function	$1(t)$	step (assumed)
Azimuth of strike	ϕ_0	330°–337° east of north
Dip of fault	δ	55°–60°
Slip angle	λ	175°–178°
Epicentral coordinates		28°23'N96°41'E
Time of origin		14: 09: 29.2 UT

With few observed data, supplemented by guiding reported data we could determine the focal parameters. It turned out, as has been often claimed for major events, that the vast energy was released through a strike-slip faulting.

The choice between the two dual planes is done on the basis of aftershock distribution, directivity and geological features of the area. The two planes strike about NNW-SSE and ENE-WSW, respectively. If we plot the first fourteen aftershocks we see that most of them concentrate on the first direction. Since we do not know how reliable are the epicenter determinations we looked at the relative times of P arrivals between stations of different azimuths - and again one is convinced that the aftershocks ran on the first direction. Moreover, the epicenter falls on a fault striking in the NNW

direction.

The Indian subcontinent is forced to move down, west and north, thus underthrusting the Himalayas in a northwesterly direction. The fault is striking NNW and dipping toward ENE. Banerji and Krishnan described the geological features as follows:

"The frontal structures of the Himalayan belt are a series of arcs convex to the south. The Burma arc is convex to the west. These two arc systems meet in the form of a hair-pin round the spot where the earthquake occurred. The trend of the mountain ranges indicates an angle of about 60° in this corner of Assam, known as the Assam wedge. This critical region is little known because of its inaccessibility."

Tectonically, we have a NNW motion of the Assam wedge on a strike-slip faulting (very little underthrusting Asia). As the seismicity of the region is diffuse, one cannot delineate the plate boundaries at the focal region. Fitch concluded that earthquakes originating under the Himalayan and the Burmese arcs, are a result of the convergence between the Indian and the Asian plates. However, he did not accoutn for the seismicity at the junction of the two arcs. Evans describes the Assam wedge independently. Hence, one is impressed that we might have there a transform-fault system in the direction of the Indian trend of motion, connecting the Himalayan edge of the Indian plate with its Burmese edge. Of course, these source parameters can be interpreted locally, by Dutta's idea of Assam's tendency of rotation.

The absolute motion of the Asian plate near the Assam wedge was given by Solomon and Sleep. It thus may appear that the simplest interpretation to the strike-slip motion on the fault of the Assam earthquake of Aug. 15, 1950 resulted from the motion of the Asian plate on one hand and the counter-motion of the Assam wedge driven by the general motion of the Indian sub-continent, on the other hand.

(b) The Siberian explosion

Old seismograms of the Tungus event of June 30, 1908 are analysed and compared with contemporary records of air explosions from Novaya Zemlya and Lop-Nor.

Observed arrival times and absolute amplitudes of Rayleigh waves, infrasonic-coupled ground-motion and SH crustal shear waves at Jena, Tiflis, Tashkent and Irkutsk, support a source model which consists of a combined action of an atmospheric-explosion equivalent to a vertical point impulse of magnitude 7.10^{18} syn sec and a ballistic-wave equivalent to a horizontal point impulse of magnitude $1.4 \cdot 10^{18}$ dyn sec striking S65°E toward the northwest.

All the accumulated knowledge in earthquake and explosion seismology since the beginning of the century is harnessed to the effort of interpreting the observed seismograms. The agreement between the observations in the eipcenteral area and the ensuing signals in the far seismic and acoustic field support the hypothesis that the Siberian UFO explosion had the effects of an Extra-terrestrial Nuclear Missle of yield 12.5 ± 2.5 Mt.

Since its occurrence on June 30, 1908, the Siberian UFO explosion has remained an unsolved mystery. Repeated efforts were made to account for this bizarre phenomenon but no single theory seems to explain all the observations. In particular, it is difficult to account for the calculated concentration of energy relase of the explosion (10^{12} erg/cm^3) which exceeds the energy concentration of known explosives by two orders of magnitude. This was perhaps the motive that forced scientists to resort to the theories of nuclear matter, anti-matter, and a black hole as the explosion-generating agent. We shall perhaps never be able to solve this problem unless a similar event reoccurs somewhere on the face of the solid earth.

However, second to the problem of the energy source there is the not

less important question of the energy carrier. The view that the Siberian UFO was a meteor of cometary origin was proposed and supported by many. Studies have shed new light on the kinematics and dynamics of the UFO and its interaction with the earth's atmosphere and surface. Combining a renewed critical evaluation and analysis of reports by eyewitnesses, the anomalous nightglow in western Europe, model experiments and, in particular, the non-symmetric felling pattern of the timber at the site of the catastrophe (some 50 km in diameter) led to the following conclusions:

(1) A meteorite (possibly a head of a comet) entered the earth's atmosphere from the southeast toward the northwest along a course 45°-65° east of the meridian with a geocentric velocity of some 40 km/sec. The inclination of the trajectory to the earth's surface did not exceed 30° and was most likely α = 15-17°.

(2) The destruction in the eipcentral zone (60°55'N, 101°57'E) could be due to the combined effect of a static explosion at height of about 5-10 km (overpressure ca. 0.06 kg/cm^2 at the boundary of the region of downthrown trees, 25 km from the epicenter) and a ballistic wave inclined at an angle α to the surface (overpressure 0.006 kg/cm^2 at 25 km from the epicenter). Extrapolation of those values to the epicenter yields an explosion overpressure of 0.7 kg/cm^2 and a corresponding yield of ca. 13 Mt (Mt = megaton).

(3) The energy liberated by the explosion was about $3 \cdot 10^{23}$ erg of which ca. $5 \cdot 10^{18}$ erg were transformed into seismic energy, thus producing a seismic event with a Richter magnitude of M = 5.0. This magnitude is also confirmed from the measurements of surface-wave amplitudes at Tashkent and Tiflis.

Thus, amplitudes and arrival times of seismic, infrasonic-seismic and infrasonic waves at stations in Eurasia, were explained in terms of a source model. The source is assumed to consist of a superpositon of an air explosion at height 8.5 km and a ballistic wave. The height of the source is deduced

from the time delay of the generation of the Rayleigh waves, relative to the time of generation of the SH body waves by the ballistic wave at Irkutsk.

This model was already proposed by Soviet astronomers a few years ago, on the basis of the timber felling pattern in the source region. Our analysis however comprises the first measurement of the far seismic field. The consistency of the near- and far-field phenomena point to the conclusion that the Siberian UFO had the effects of an extraterrestrial nuclear missile of yield 12.5 Mt.

(c) The Chinese and Soviet atmospheric explosions

Observed P and S waves from the respective Soviet and Chinese atmospheric explosions of October 30, 1961 and October 14, 1970 are found to differ both in their S/P amplitude ratios and the form of the individual wavelets. This difference is attributed to the effect of the local topography on the ensuing ground motion at the source. Asymptotic ray theory indicates that an additional horizontal force component was acting at the source of the Chinese event while the Soviet event could be modeled by a vertical force only.

Generalized ray theory is then applied to calculate the body wave forms in each case. The agreement between the theoretical results and the observations is excellent.

Surface waves excited by atmospheric nuclear exposions (ANE) were observed and studied by many investigators. Amplitudes of body waves generated by ANE are, however, much smaller and usually are harder to observe and analyze. As a result they were subjected to fewer studies.

Several source models were proposed in the theoretical studies of ANE-generated seismic waves. One of the most widely accepted source representations is essentially that of a vertical concentrated force or a radially expanding distribution of vertical forces caused by the overpressure loading of the crust. This model accounts successfully for several observations: P body

waves, Rayleigh surface waves and the absence of both SH and Love waves in the ANE-generated seismograms. In all previous ANE records known to us, P-wave amplitude was always larger than the corresponding S amplitude. However, the Chinese ANE of October 14, 1970 generated, at the WWNSS stations of SHL, QUE, CHG and MSH, S_z amplitudes which superceded those of P_z by a factor of about 2.5. This report covers these observations in detail and provides an adequate interpretation.

The amplitude excess of P over S in most ANE-generated seismograms is in agreement with the simple model of a vertical point force acting on the surface of a homogeneous half-space. Such a simplified model cannot be used, for examle, at distances of 20° where a more refined theory is needed.

The generalized ray method was used by us to calculate theoretical seismograms for a vertical concentrated force acting on the surface of a multilayered earth. It exhibits the Uppsala LP-Z recording of the Soviet ANE of October 30, 1961. The agreement of our calculation with the observation, which is quite typical, is good enough to justify both the method of calculation and the assumptions involved. Additional calculation made by us for other epicentral distances also yielded the same result, namely a P_z amplitude which is larger than the S_z amplitude.

The Chinese ANE of October 14, 1970 (40.9°N, 89.4°E), USCGS) yielded body waves at a number of stations which differ considerably in their wave forms from the corresponding phases of the above-mentioned Soviet event. Of the 40 WWNSS long-period seismograms available to us, body waves were clearly visible at four stations. There, the peak S/P amplitude ratio at 20 sec was about 2.3 to 3.0 The same phenomenon was observed in records of the Chinese event of July 17, 1967 (40.7°N, 89.6°E, USCGS). The repeatability of the records, under similar conditions, tends to support our hypothesis. The seismograms of both Chinese events could not be explained

by means of a vertical point force. However a glance at a topographical map of the source region shows it to be a mountainous area which cannot be approximated by a flat boundary. It seems, therefore, that a proper description of the force acting on the earth, due to the overpressure of the ANE, should be that of a force perpendicular to the earth's surface at the vicinity of the source. Thus, when a plane-parallel layering is assumed, the net force exerted on it by the ANE is inclined to the idealized surface, the angle depending on the true topographical features of the source area. This force can be decomposed into vertical and horizontal components.

2. Seismicity, Tectonics and Structure of the Near East (A. Ben-Menahem, A. Nur and M. Vered)

The purpose of this study was to unveil the tectonics and seismicity, S-wave velocity structure and inelastic behaviour with depth of the earth's crust in the continental Near-East. To this end, we have analyzed body wave phases and surface wave signals from 47 earthquakes in the magnitude range 3 1/2 - 5 1/2 that were originated and recorded in (or close to the margins of) the Near-East during 1927-1974. Initial motions, P and S wave-forms, radiation patterns of crustal Love and Rayleigh waves, spectral amplitudes, dispersion and travel-time data as well as geologic, morphologic and historical data were used in unison to provide information on tectonic patterns, slip rates and the inelastic properties of the crust. Most of the numerical algorithms and inversion routines that have been generated during the computer era were utilized. In this sense, this is the first experimental effort in which both amplitude and phase data were simultaneously inverted over a broad frequency range to yield information on both source and structural parameters in one stroke

We found a rather sharp Moho discontinuity with average thickness of 32-35 km underlaying the continental crust. The crust contains cracks and pressurized water to a depth of about 20 km. Below this depth the rock becomes ductile. This acounts for a confinement of seismic activity in the upper crust, the low-values of Poisson's ratio (0.18-0.21) at 20-25 km and the low Q values there.

Crustal shear velocities in Sinai and the Levant fracture zone are significantly higher than the corresponding velocities in the eastbound section Eilat-Zagros foothills.

Fault plane solutions and kinematic source parameters of 15 earthquakes since 1927 together with a critical examination of historical seismicity during the last 4000 years, were used to unveil the major tectonic features of the junction zone. The main results are:

(1) The fault systems in the Afro-Eurasian junction (apart from its northern end) have a dominantly left-lateral strike-slip component, transforming the opening motion of the ridge-like Red Sea into a collision zone of the Alpine mountain belt. In this region the edges of the coherent Arabia and Africa plates break up in the neighbourhood of their boundary as they approach the region of continental collision with the Eurasian plate. This breakup consists of gradual loss of coherency and deterioration of its rigidity as more and more deformation is taken up by the branching faults.

(2) The Sinai region should not be considered a separate plate, but rather a splinter of the Africa plate, which is breaking up incoherently as it approaches the zone of collision. It is probably useless to try to find its western boundary.

(3) The Dead Sea fault - a source for many Biblical and post-Biblical earthquakes in the last four millenia - was definitely identified. It has an estimated mean rate of activity of 2 events/century at magnitudes from 5 to 7. An aseismic slip rate of 3 mm/year is taking place along this fault.

A full-size report is attached herewith.

(3) Theoretical Seismograms for Real Earth and Source Models and its Applications (A. Ben-Menahem and M. Vered)

New numerical methods were developed which enable us to simulate on the Institute's computers recording of ground motion from real seismic events. The following factors are taken into account in the generation of the seismogram: 1) the vertical structural heterogeneity of the earth's crust and upper mantle; 2) instrumental distortion; 3) attenuation; 4) source of arbitrary spatial and temporal dependence (shear dislocation in particular).

Extensive efforts are being made to include constant gradients and the earth's sphericity. Data, in digital form, are supplied by our V.rian 8K computer oeprating in the Alopho Bloch Geophysical Observatory.

We are successful in generating seismograms from a realistic source model of regional earthquakes. A good agreement between syntehtic and observed wave forms from a source at $\Delta = 17°$ proves this method to be useful for studying either the structural parameters or the source parameters when the others are known.

An alternative method for the computation of seismograms for surface and shallow sources was developed.

A generalized multipolar ray theory (GMRT) is presented. It incorporates multipolar source theory and extended versions of both the Cagniard-Pekeris method and Spencer's prescription. The multipolar source theory is developed in an attempt to give a unified and systematic representation of seismic sources. The results of Cagniard-Pekeris and Spencer are extended on three levels, by:

(1) Formulating and proving the applicability of the Cagniard-Pekeris method to non-symmetric earthquake sources of arbitrary multipolar order, with a particular emphasis on shear dislocations;

(2) Showing that Spencer's prescription for propagating disturbances across planar interfaces holds for multipolar sources in a layered half-space;

(3) Giving a rigorously justified procedure for propagating disturbances across spherical boundaries.

The resultant GMRT enables one to compute the exact time domain response of any point in a multilayered sphere or half-space to the action of a buried multipolar point source. Ad-hoc versions of GMRT specially suited for near field and shallow source studies are derived.

The analytic expressions of GMRT are exactly decomposed into constituents which are identified as head-waves, reflected waves and non-least time path arrivals. This physical interpretation is carried out using both kinematic and dynamic characteristics of the field entities. Computational and numerical schemes which facilitate the synthesis of seismograms by GMRT are presented.

GMRT is applied to investigate source mechanisms of diverse geophysical phenomenon. Some of these are: small and intermediate earthquakes in the near, intermediate and far field, atmospheric nuclear explosions, the Siberian meteor of 1908 and surface sources. It is found that:

(1) Source radiation pattern effects can be successfully taken into account by GMRT studies;

(2) Both magnitude and fault plane solutions obtained by GMRT are concordant with the results obtained by classical methods;

(3) Source parameters may be evaluated from near field measurements;

(4) Atmospheric nuclear explosions need be represented by both vertical and horizontal point forces. The dip angle of the resultant force depends on local topography in the epicentral area. In particular, the excess of S over P amplitude observed in records of Chinese events, is explained by this model;

(5) Source parameters of small earthquakes in the northern Red-Sea region lie in the range $285 \leq \lambda \leq 319$, $34 \leq \delta \leq 55$, $245 \leq \theta \leq 352$. It is consistent with previous seismological studies of the same area;

(6) The motion along the Dead-Sea rift is of left-hand shear type;

(7) The source parameters of the Iran earthquake of Feb. 23, 1970 are $\lambda=62$, $\delta=42$, $\theta=287$, $h=25$km. It is in agreement with the tectonics of the southern Zagros Zone;

(8) The source mechanism proposed by Ben-Menahem to describe the Siberian meteor of 1908 is confirmed by GMRT considerations. Only one of several crustal medels of the siberian plateau is consistent with the data.

Seismological data, obtained in the form of seismograms, can be processed and interpreted in either the frequency or the time domains. The first step in frequency domain analysis is usually that of Fourier transforming the raw data. This is quite a costly procedure, justified only by the relative ease of the following manipulations of the data. Time domain studies do not need this first step. However, the mathematics involved in such analysis is much more difficult to derive and apply. As a result frequency domain techniques became the tools more frequently used by seismologists. In recent years, however, much attention began to be paid to time domain studies, focusing in particular on the concept of theoretical seismograms.

The basic idea of using synthetic seismograms is to compare computed seismograms directly with observed ones. One can change the theoretical models or assumptions involved in the synthesis of the seismograms till agreement with observations is acheived. The final theoretical model is necessarily an adequate description of the true physical phenomenon under investigation.

Several methods of synthesizing seismograms were developed. Most notable are those using the concepts of asymptotic ray theory, reflectivity, and generalized ray theory. The generalized ray theory (henceforth refered to as GRT) seems to be by far the most powerful and accurate method to date.

GRT is based largely upon the work of Cagniard, Pekeris and Spencer. The fundamental aim of GRT is to describe the time domain response of two elastic half-spaces which are in welded contact along a plane boundary, to a point source embedded in one of the half-spaces. The exact classical solution of this problem is written as a double integral where one integration is over the separation variable, and the other over the time-transformation variable. The integrand, in turn, contains a Bessel function, which may be represented by yet an additional integration. This triple integral can be treated only approximately over certain limited regions. Cagniard and Pekeris showed, independently, that by suitably distorting the integration contours, two integrations in the triple integral may be played against each other to the point of their mutual annihiliation. The resultant expression consists of a single integration which may be carried out either analytically, as in the case of surface sources, or numerically, as in the case of buried sources.

Direct extensions of the Cagniard-Pekeris method to layered media were undertaken by several investigators. Mencher solved the problem of epicentral displacement in an infinite slab. Pekeris et al. dealt, under somewhat restricting conditions, with the propagation of a compressional pulse in a layer overlying a halfspace. Abramovich reinvestigated, and significantly extended, a similar but more general problem. Any further progress along the same lines towards solving the multilayered case seems to be impractical.

A new line of attack was opened by combining a variant of the Cagniard-Pekeris and Spencer methods. Spencer introduced the idea of generalized rays in a multilayered media. He used this idea to give a prescription for the propagation of the integral representation of the disturbance along the path of the generalized ray. Although Spencer apparently considered the possibility of linking his and Cagniard's results, he limited his applications to the frequency domain only. It was Sherwood and Helmberger who welded these two tools to form the GRT.

The use of GRT in seismology is quite restricted. A handicap of GRT is that both its constituents, the Cagniard-Pekeris and the Spencer methods are limited to plane parallel models. Such a model may be a good enough approximation of that part of the Earth through which seismic waves propagate to short distances, but is certainly unapplicable at large distances.

A more serious disadvantage, from the seismological point of view, of GRT is that it applies to symmetric sources only. Cagniard's work dealt with a radially symmetric source, while Pekeris initially considered an axially symmetric source, the vertical concentrated force.

Later, he investigated a horizontal torque pulse and, with others, made a study of an SH torque. Muller dealt with single forces and double couples. All these sources can not adequately describe earthquake sources. Moreover, Spencer's prescription, so vital for GRT, was derived for axially symmetric sources only.

The use of GRT is further restricted by the fact that most of the computational and numerical methods used for synthesis of seismograms, were developed with an explosion source in mind. For example, the initial motion approximation involves an approximation, which is exact for explosions, but

amounts in certain cases, to some 20% of the final result for strike-slip sources. Another example is ray enumeration which was developed for surface sources but is certainly unapplicable for buried sources, such as earthquakes' are.

We were thus confronted with the formidable task of formulating a generalization of GRT, which would apply to earthquake sources in real earth models. We called this comprehensive theory 'generalized multipolar ray theory' abbreviated to GMRT. The five main objectives were to extend:

(i) The Cagniard-Pekeris method to multipolar sources;

(ii) The Spencer prescription to multipolar sources;

(iii) The Cagniard-Pekeris method to a homogeneous sphere;

(iv) The Spencer prescription to a layered sphere;

(v) Computational and numerical methods to realistic earthquake sources.

Four of these five objectives are dealt with in this work. The fifth, that of extending the Cagniard-Pekeris method to a homogeneous sphere is circumvented. Following Chapman and Helmberger the sphere is approximately 'flattened' and objective (iii) is then trivially attained.

The usefulness of GMRT in seismological studies can not be overemphasized. It is a comprehensive, almost assumptions free theory which is equally easily adaptable to near and far-field studies, short and long periods, interfering or distinct waveforms and surface or buried sources. As a result it may be used as a research tool in many diverse phenomenon.

(a) Extension and interpretation of the Cagniard-Pekeris method for dislocation sources

A variant of the Cagniard-Pekeris inversion technique is extended to nonsymmetric earthquake sources of arbitrary multipolar order with a particular emphasis on shear dislocations. In the present work, we concentrate on the infrastructure of the time-domain displacement field in the presence of a single interface. A series of transformations in the complex plane together with a novel decompositon of the total field into three fundamental constituents enables us to separate the real-time contributions due to head waves, geometrical waves and the so-called non-least-time arrivals.

The Cagniard-Pekeris method of obtaining the time-dependent response of two elastic half-spaces in welded contact along a plane boundary was originally developed for a symmetric point source. Cagniard's work deals with a radially symmetric point source, while Pekeris initially considered an axially symqetric point source, the vertical concentrated force. Later, he investigated a horizontal torque pulse and, with others made a study of an SH-torque. Muller dealt with single forces and double couples. To the best of our knowlege, this method has not been applied to point sources in general. In the present work, we extend this theory to include all multipolar point sources. Dislocation sources are extensively treated and all field components due to them are tablulated. The treatment is quite general, and while solid/solid interface terminology is used, the appropriate coefficients for other types of interfaces are given as well. The final result of the extended Cagniard-Pekeris method is exactly decomposed into three constituents: head waves, geometrical reflected waves and the so-called non-least-time path waves. The identification of the first tow terms by their kinematic characteristics is well known; but the dynamic identification in the time domain is not as generally known.

The decompositon effected by Dix is useful for the vertical longitudinal part of the displacement. His method, following Cagniard, is that of breaking up the P-P reflection coefficient and identifying each contribution along the appropriate integration path. This method is not automatically extended to other types of reflection, and the physical meaning of his "Psuedo-reflected" waves is interpreted in our work. Our method is more general and is applicable in a straightforward manner to all cases. Our results concerning the third term in the above mentioned decomposition agrees qualitatively with those of Lapwood which were derived in the frequency domain.

(b) Application of synthetic seismograms to the study of low-magnitude earthquakes and crustal structure in the northern Red Sea region

Previous theoretical results are used to produce synthesized seismograms for realistic crustal models and earthquake dislocation sources. Short-period vertical displacement seismograms at Δ = 240 km are calculated. They show strong resemblance to observed recordings, at least for the first 55 sec after the P_n arrival. These results are then used for the study of low-magnitude earthquakes from a known source and the tectonics of the source region south of the Sinai peninsula. The source-mechanism found by Ben-Menahem and Aboodi and the crustal structres given by Niazi and Drake and Girdler are consistent with the time series of many short-period seismograms recorded at Eilat since 1969.

Much attention has been paid in recent years to the computation of theoretical seismograms and its application to geophysical studies. Several methods were developed employing the concepts of generalized rays, reflectivity, and asymptotic ray theory. Asymptotic ray theory contains no assumptions concerning the radiation pattern of the source, wehreas the other two

methods mentioned above were developed and used for axially symmetric point sources only. In a recent work the Cagniard-Pekeris technique was extended to multipolar point sources, embedded in one of two half-spaces in welded contact along a plane boundary. In the present work we have extended our former results to multilayered half-space models, thus providing a useful method of generating synthetic seismograms for realistic earthquake sources. A method of decomposing the resulting expressions is described and a critical comparison with other methods is presented. Efficient methods of generating and enumerating multireflected rays are suggested, based in part on the work of Hron. Using these computational procedures, synthetic seismograms for the four fundamental dipolar sources are presented. We have computed these seismograms for the whole time interval dominated by body waves, whereas previous workds dealt almost exclusively with the pure P-wave contribution (barring, of course, treatment of surface waves). Comparison between theoretical seismograms and observed ones is presented and discussed.

(c) Computer generated P and S waveforms from an earthquake source

Theoretical seismograms are calculated for a realistic source model at $\Delta = 17°$. Both P and S groups are synthesized at the stations EIL and JER, from an earthquake of magnitude 5.5 in Iran.

It is shown, using a course structural model, that good agreement between synthetic and observed waveforms can be obtained when radiation pattern effects are theoretically taken into account.

This agreement gives hope that the present method could be used to study either structural or source parameters when the other is known.

In most source mechanism and earth structure studies, one usually utilizes only a small portion of the information that is carried by the P and S body waves. The method of generalized rays (GRT) seems to enable

one to compare the entire observed and synthetic waveforms. Early studies along these lines were limited to axially symmetric sources only, mainly explosion sources. Recently, Ben-Menahem and Vered combined the GRT and source theory to a unified tool which we shall call GMRT (generalized multipolar ray theory). The application of GMRT to earthquake sources is quite straightforward. Vered and Ben-Menahem were first to apply GMRT to earthquake mechanism and earth structure studies. Other investigators tried to avoid the use of GMRT, e.g. by applying modifications of GRT to such cases where radiation pattern effects were minimal.

The aim of the present study is to demonstrate the feasibility of generating synthetic seismograms for a realistic earthquake source which agree with observations. The data used are the long period vertical WWNSS records from JER (Δ = 17.2°) and EIL (Δ = 17.3°) of an earthquake in Iran (23 February, 1970; 11h22m28.5s; epicentre at 27.8°N, 54°.5°E; mag = 5.5).

The coupling of the source theory to GRT is shown to be a powerful tool in generating realistic synthetic seismograms. Moreover, the approximations applied to the original GRT results (e.g. first motions, asymptotic expansions, etc.) may be implemented after the source effects have been taken into account. Thus, it seems that radiation pattern effects should not be avoided in future studies by GRT.

(d) Generalized multipolar ray theory for surface and shallow sources

The study of surface and shallow sources has lately become of importance, especially in connection with nuclear-explosion seismology. An ad-hoc study of surface sources was deemed necessary in view of the observation that, in general, the radiation pattern of a surface source differs substantially from the radiation pattern of the same source buried in an infinite space. Consequently, an exact generalized multipolar ray theory (GMRT) is developed

for surface sources. This theory holds but approximately for buried sources. However, for shallow sources the approximation is quite acceptable, while making the tedious evaluation of surface reflections redundant. The same problem of computing theoretical seismograms for shallow sources was recently investigated, in an approximate way, by Langston and Helmberger.

Radiation patterns of surface sources may be derived in different ways; ab initio solution of a surface source problem , or finding the radiation field of a buried source and taking the limit as the burial depth tends to zero. We use a version of the second technique. The direct and reflected displacement fields for buried multipolar sources were given in detail by Ben-Menahem and Vered. We form the total field by adding the direct and reflected fields. The resultant expression may be expanded in a Taylor series in a non-dimensional quantity which eventually may be shown to be kh where k is the wave number and h the burial depth of the source. Asymptotic ray expressions may be obtained by approximately evaluating the exact field entities using the stationary phase method and the initial motion approximation. The two main advantages of our method are that: (1) it applies equally easily to all multipolar sources, thus avoiding the need to re-evaluate the radiation pattern anew for every source, and (2) it may be straightforwardly applied to multilayered media.

The first term in the above mentioned expansion yields the radiation pattern for surface sources. The second term in the series may be considered as a correction to be added to the first term, for small non-vanishing h, and so on.

(e) Generalized reflection and transmission coefficients for seismic sources in a multi-layered spherical earth model

A method of propagating the components of the displacement across interfaces in a multi-layered spherical earth model is presented. It is useful both for explosion sources and tangential dislocation sources, buried in an arbitrary layer of the model. Combined with known techniques, our method yields a useful tool for generating synthetic seismograms for earthquake sources in realistic earth models.

The Cagniard-Pekeris method of obtaining the time-dependent response of two elastic half spaces in welded contact to point dislocation sources was combined with Spencer's prescription of generalized reflection/transmission coefficients. This method enables one to generate synthetic seismograms for multipolar sources in a multi-layered half-space. In the present work, the use of Spencer's method for a layered sphere is rigorously justified, and is further extended to tangential dislocation sources buried in an arbitrary layer of the model.

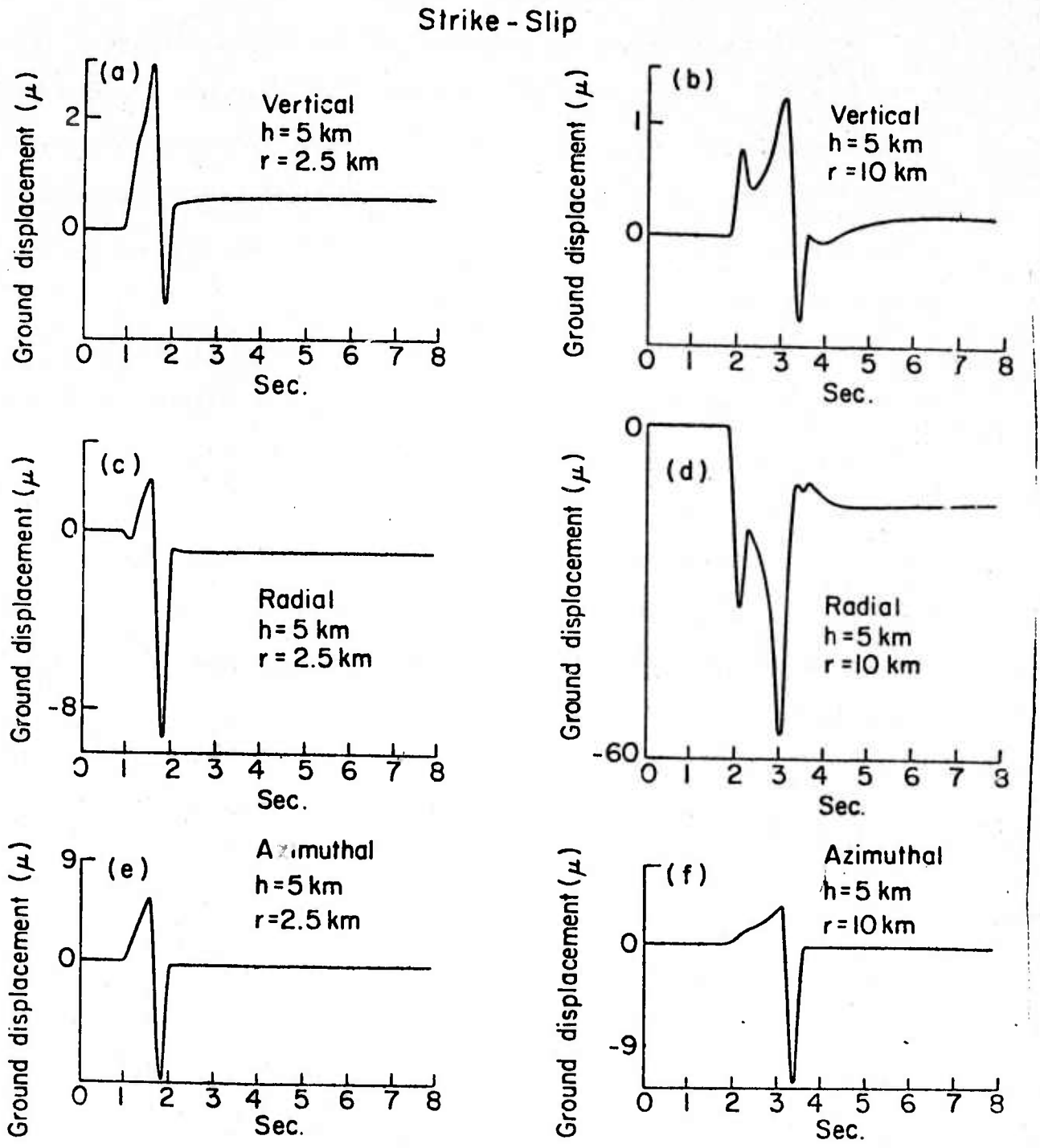
Strike - Slip
(a)
Vertical
h = 5 km
r = 2.5 km
Ground displacement (μ)
2
0
0 1 2 3 4 5 6 7 8
Sec.
(b)
Vertical
h = 5 km
r = 10 km
Ground displacement (μ)
1
0
0 1 2 3 4 5 6 7 8
Sec.
(c)
Radial
h = 5 km
r = 2.5 km
Ground displacement (μ)
0
-8
0 1 2 3 4 5 6 7 8
Sec.
(d)
Radial
h = 5 km
r = 10 km
Ground displacement (μ)
0
-60
0 1 2 3 4 5 6 7 8
Sec.
(e)
Azimuthal
h = 5 km
r = 2.5 km
Ground displacement (μ)
9
0
0 1 2 3 4 5 6 7 8
Sec.
(f)
Azimuthal
h = 5 km
r = 10 km
Ground displacement (μ)
0
-9
0 1 2 3 4 5 6 7 8
Sec.

Fig. 1

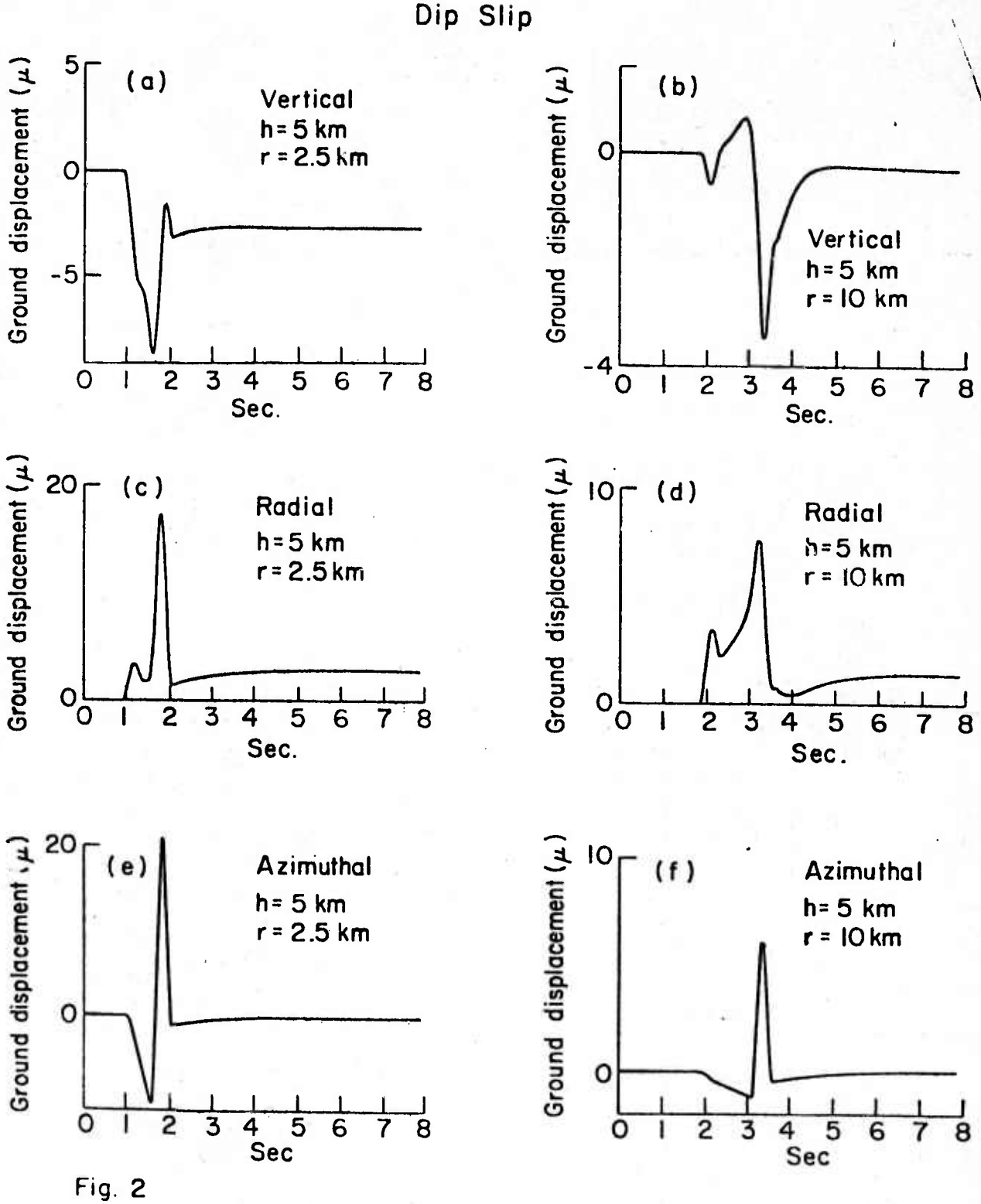
Dip Slip
(a)
Vertical
h=5 km
r=2.5 km
Ground displacement (μ)
5
0
-5
0 1 2 3 4 5 6 7 8
Sec.
(b)
Vertical
h=5 km
r=10 km
Ground displacement (μ)
0
-4
0 1 2 3 4 5 6 7 8
Sec.
(c)
Radial
h=5 km
r=2.5 km
Ground displacement (μ)
20
0
0 1 2 3 4 5 6 7 8
Sec.
(d)
Radial
h=5 km
r=10 km
Ground displacement (μ)
10
0
0 1 2 3 4 5 6 7 8
Sec.
(e)
Azimuthal
h=5 km
r=2.5 km
Ground displacement (μ)
20
0
0 1 2 3 4 5 6 7 8
Sec
(f)
Azimuthal
h=5 km
r=10 km
Ground displacement (μ)
10
0
0 1 2 3 4 5 6 7 8
Sec

Fig. 2

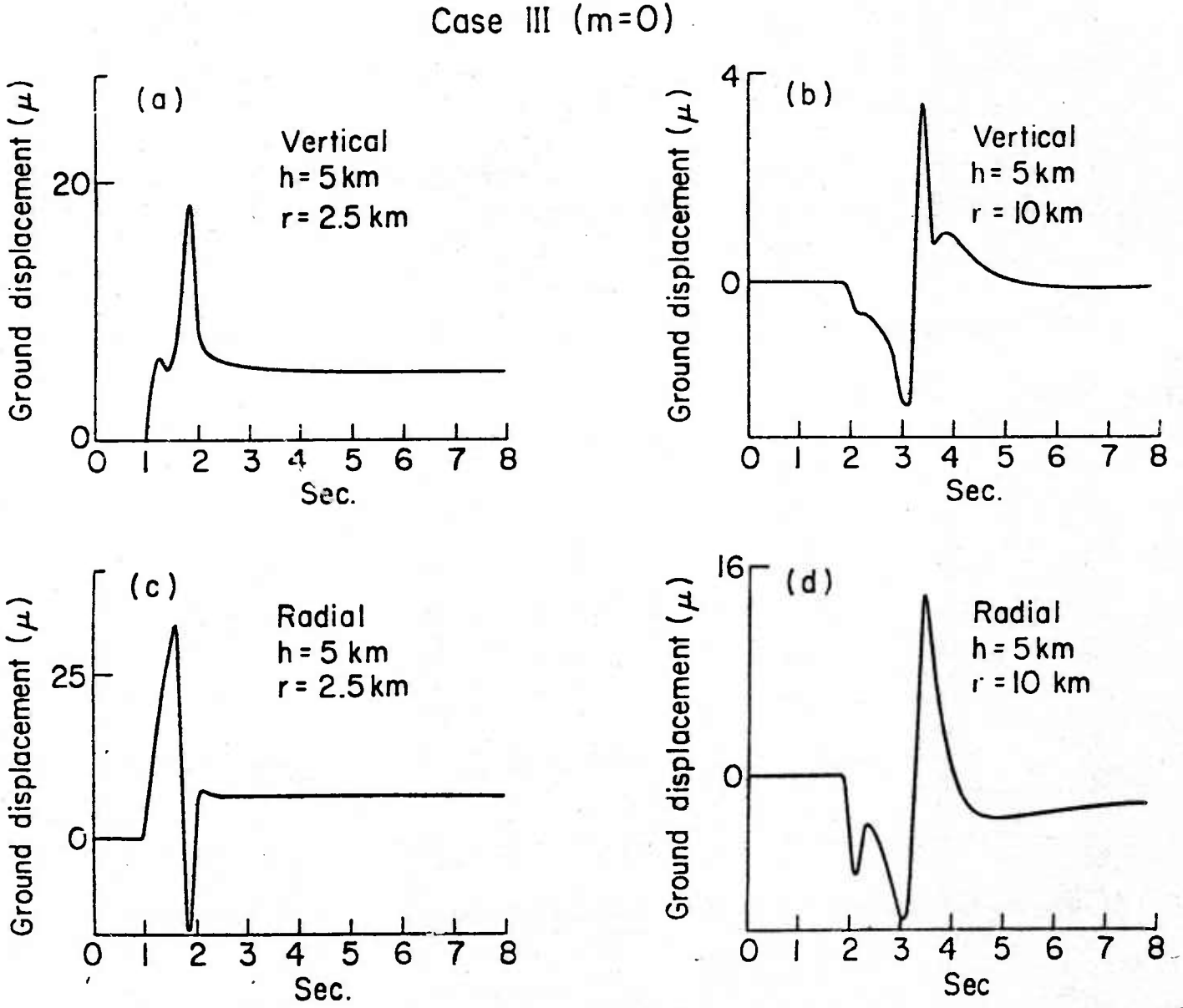
Case III (m=0)
(a)
Vertical
h= 5km
r= 2.5 km
Ground displacement (μ)
20
0
0 1 2 3 4 5 6 7 8
Sec.
(b)
Vertical
h= 5km
r = 10km
4
0
Ground displacement (μ)
0 1 2 3 4 5 6 7 8
Sec.
(c)
Radial
h= 5 km
r= 2.5km
Ground displacement (μ)
25
0
0 1 2 3 4 5 6 7 8
Sec.
(d)
Radial
h= 5km
r = 10 km
16
0
Ground displacement (μ)
0 1 2 3 4 5 6 7 8
Sec

Fig. 3

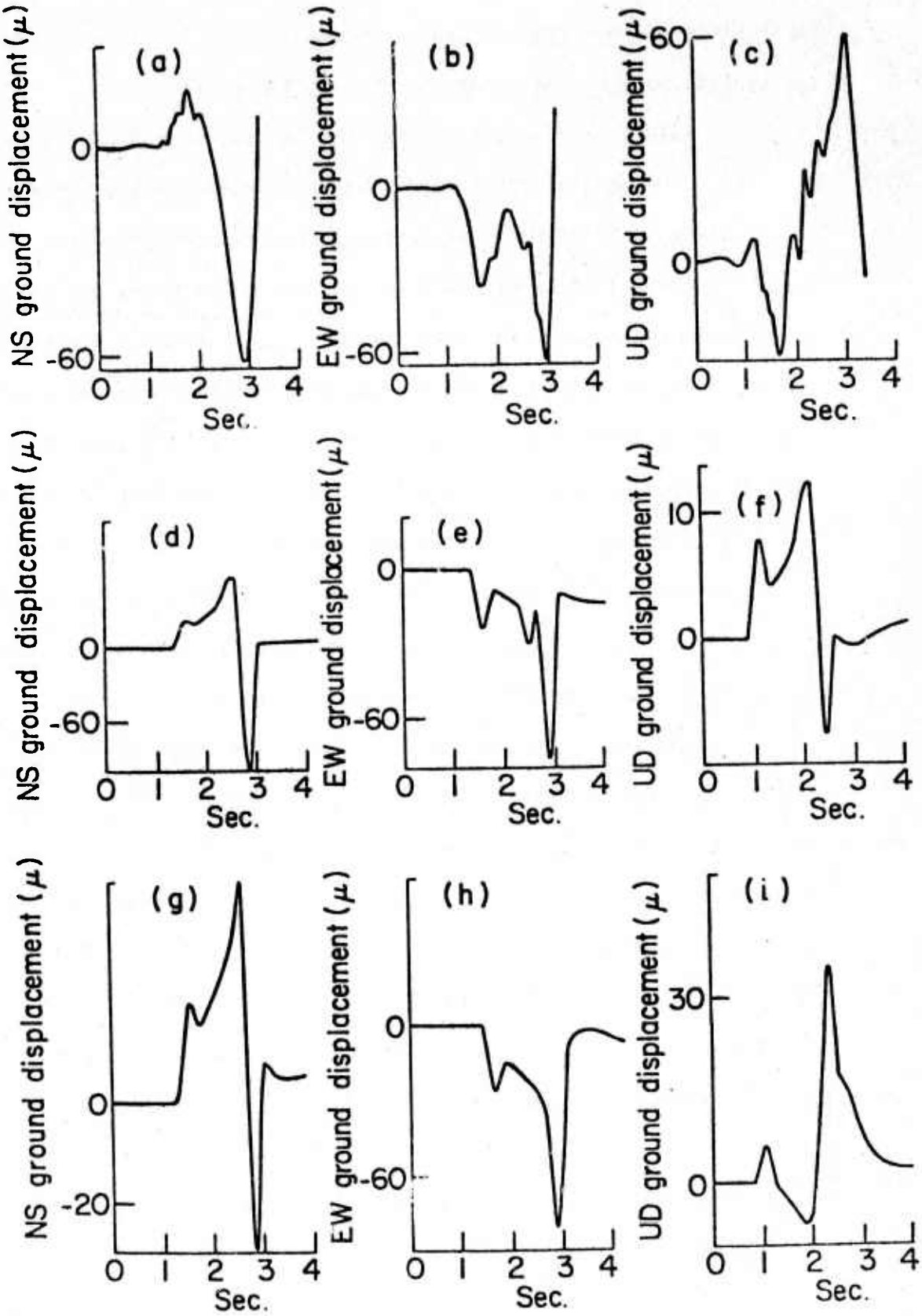
(a)
NS ground displacement (μ)
0
-60
0 1 2 3 4
Sec.
(b)
EW ground displacement (μ)
0
-60
0 1 2 3 4
Sec.
(c)
UD ground displacement (μ)
60
0
0 1 2 3 4
Sec.
(d)
NS ground displacement (μ)
0
-60
0 1 2 3 4
Sec.
(e)
EW ground displacement (μ)
0
-60
0 1 2 3 4
Sec.
(f)
UD ground displacement (μ)
10
0
0 1 2 3 4
Sec.
(g)
NS ground displacement (μ)
0
-20
0 1 2 3 4
Sec.
(h)
EW ground displacement (μ)
0
-60
0 1 2 3 4
Sec.
(i)
UD ground displacement (μ)
30
0
0 1 2 3 4
Sec.

Fig. 4

(4) Problems of Wave Propagation (A. Ben-Menahem)

(a) Elastic wave-motion across a vertical discontinuity

Exact solutions are obtained for the displacement field in an elastic half-space composed of two quarter spaces welded together. The configuration is excited by a plane SH wave impinging upon the discontinuity at an arbitrary angle. The application of the Kontorovich-Lebedev transform to this boundary value problem leads to two simultaneous integral equations which are solved exactly. It is shown that the discontinuity may enhance the spectral displacements up to a factor of two. The results could be applied to propagation of seismic shear waves past fault zones in the earth's crust.

In recent years considerable interest has been shown by many investigators to the propagation of elastic waves in parallel layered media. The techniques developed for such configurations can model only vertical heterogeneities while solutions to problem s involving lateral structural variations in elastic media are almost unknown. The reason is that the boundary conditions equations in layered media are reduced to a set of algebraic equations while the other types of non-homogeneity involve ab initio integral equations for the reflection coefficients. Certain approximations are sometimes helpful, but useful working tools are still lacking in as much as the ensuing integral equations are not text-book items.

The interaction of elastic waves with dipping discontinuities is a problem which belongs to the above category. We have found however that for a vertical dip angle a solution is attainable in a closed form. It is hoped that these results could be generalized to more complicated physical regimes.

(b) Properties and applications of a certain operator associated with the Kontorovich-Lebedev transform

The integral

$$Q(r,m) = \int_0^\infty K_{i\tau}(\beta_1 r) k_{im}(\beta_2 r) \frac{dr}{r}$$

arises in problems of scalar wave propagation in welded elastic wedges. $K_{im}(\beta_1 r)$ is the modified Bessel function of the second kind and m,τ are real. It is shown that $Q(\tau,m)$ is a generalized function that includes a complex shift operator. We shall investigate the properties of this operator and establish a new integral transform based on the kernal $Q(\tau,m)$.

A summation formula based on $Q(\tau,m)$ is derived, which facilitates the evaluation of sums involving the Jacobi polynomials. Finally, $Q(\tau,m)$ is used to obtain a new multiplication theorem for the MacDonald functions.

(5) List of Publications

1974 Generalized reflection and transmission coefficients for seismic sources in a multilayered spherical earth model, Pure and Appl. Geoph ., v. 112, p. 831-835.

1974 Changes in the earth's inertia tensor due to earthquakes by MacCullagh's formula, Geophysical Journ., v. 40, p. 289-274.

1974 The source of the great Assam earthquake - an interplate wedge motion, Phys. Earth. Plan. Int., v. 9, p. 265-289.

1975 Elastic wave-motion across a vertical discontinuity, Journ. of Engineering Mathematics, v. 9, p. 145-158.

1975 Computer generated P and S waves from an earthquake source,, PAEG, v. 113, p. 651-659.

1975 Modeling of atmoshperic nuclear explosions over a mountainous region by vertical and horizontal single forces, Bull. Seism. Soc. Am., v. 65, p. 971-980.

1975 Source parameters of the Siberian explosion of June 30, 1908 from analysis and synthesis of seismic signals at four stations, Phys. Earth. Plan. Int., v. 11, p. 1-35.

1975 Properties and applications of a certain operator associated with the Kontorovich-Lebedev transform, Proc. Glasgow Math. Assoc., v. 16, Part II, p. 109-122.

1976 Tectonics, seismicity and structure of the Afro-Eurasian junction, Phys. Earth Plan. Int. (in press)

1976 Ceneralized multipolar ray theory for surface and shallow sources, Geophys. Journ. Roy. Astr. Soc., v. 45, p. 1-4.

(a)

TECTONICS, SEISMICITY AND STRUCTURE OF THE AFRO-EURASIAN JUNCTION - THE BREAKING OF AN INCOHERENT PLATE

by

ARI BEN-MENAHEM,

AMOS NUR and MOSHE VERED

Adolpho Bloch Geophysical Observatory
Department of Applied Mathematics
The Weizmann Institute of Science
Rehovot, Israel

and

Department of Geophysics
Stanford University
Stanford, California 94305

October 1975

1. INTRODUCTION

The geographical zone bounded from the east and north by the Zagros-Taurus belt, from the west by the Mediterranean continental shelf, and from the south and southeast by northern Arabia, Sinai and the Nile delta, is named by us the Afro-Eurasian junction. Its tectonics, unlike most other active seismic zones in the world, has been reflected in many historical records since the dawn of civilization. Chief among them is the Bible, in which we find distant echos to tectonic events as remote as 2000 B.C. No one has expressed this in greater clarity than Dr. Bailey Willis (a pioneer seismologist of the Holy Land, 1857-1949) in his well-known paper "Earthquakes in the Holy Land" (1928):

"From times immemorial Palestine and Syria have been afflicted by earthquakes. Not that there is precise statement of fact in ancient writings; it is not to be expected that the people of antiquity would have had or could have preserved definite records, but there are many references in the traditions from which Old Testament history sprang, and in the Old Testament itself, which either suggest the occurrence of earthquakes or state clearly the fact of their occurrence."

Lists of earthquakes that include most dates of occurrence and names of cities closest to the epicenter have been compiled from many and diverse sources by Willis (1928), Sieberg (1932, 1932a), Amiran (1951) and Ambraseys (1962). These lists, although being inaccurate and incomplete in details, include probably the major seismic events that took place in the area during the past 2000 years. Since the epicenters are known with poor accuracy, the lists can only serve as an overal zonal measure of seismicity. Perhaps the most important piece of information that one may deduce from the aforementioned lists is the occurrence of about 40 intermediate and major earthquakes

(M = 5-7) in the Levant fracture zone during the past 20 centuries, yielding an average "quiet" interval of 50 years. Somewhat more than the day of occurrence, and a rough measure of intensity (which characterizes most of the list's items) is offered through the isoseismals of Sieberg (1932). Some of his plots are exhibited in Fig. 1. Numerals therein refer to the Mercelli-Cancani scale. Fig. 2 shows the effect of the earthquake of Nov. 25, 1759 upon the remains of the Baalbek temple of Bacchus. The isoseismals are the first experimental verification that the major faulting systems in the Levant fracture zone are oriented in the NNE-SSW direction. The compilations of Arieh (1967) and Karnik (1969, 1971) show similar trends. However, since the accuracy of their epicenter location is ± 30 km on the average, no clear delineation of epicenters could be made.

The advent of the new plate tectonics (Le Pichon et al., 1973) gave new impetus to tectonic studies of the Mediterranean area and the Middle East. Ben-Menahem and Aboodi (1971) presented for the first time seismological evidence for the relative motion of the African and the Arabian plates and the left lateral motion along the Jordan rift valley. Moreover, it was found that there is also a left lateral strike-slip component of motion along the Gulf of Suez. Nowroozi (1971, 1972) produced a merger of geological maps, epicenter locations and fault plane solutions based upon short-period readings of first motions (Shirokova, 1967; Wickens and Hodgson, 1967) in an effort to obtain general tectonic features of the Middle East. His data were however insufficient to draw definitive conclusions on the tectonics of our region of interest.

We are thus faced with a situation in which we have overwhelming evidence for historical seismicity and massive geological evidence for surface fracture

almost everywhere along the rift valley, while we are unable to answer such simple questions as:

- What is the crustal structure in the near-east?
- What is the source of tsunamis which have hit repeatedly at the coasts of Israel, Syria and Lebanon during historical times?
- Where are the seismically active faults in the Afro-Eurasian junction and what is the direction and rate of slip on them?
- What is the direction of motion along the Jordan rift zone? Is it purely strike-slip fault, as predicted by plate tectonics, and suggested by geological evidence?

Such questions and others are of regional significance and also have important global implications. Furthermore, the Jordan rift valley and the Gulf of Eilat are both parts of the boundary between the Asian plate and the African plate. It is one of the rare places on earth where the boundary is actually exposed on a continent and not buried under the ocean.
An overall tectonic interpretation must tie up with global plate tectonics on one hand and with local geological infrastructure and historical seismicity records on the other hand. To achieve these objectives we shall use all available seismograms of most major seismic events that occurred in the area in recent years. Because of the scarcity of good, reliable data special efforts will be made to utilize the entire seismogram including crustal reflections and refractions. The magnitude range of the available events (M = 3 1/2 - 6 1/2) and the linear dimensions of the propagation paths (200-2000 km) dictate the use of surface waves in the intermediate period range 10 - 50 sec.

Previous efforts to harness crustal Love and Rayleigh waves for source studies begin with Gutenberg (1955) who was first to notice the strong effect

of the radiation-pattern via the azimuthal dependence of the magnitude (!) at T = 20 sec. Aki et al. (1969) and Canitez and Toksoz (1972) utilized theoretical spectra of crustal surface waves in their source mechanism studies of certain California earthquakes. Brune and Allen (1961) and Wyss and Brune (1968) treated the dependence of the potency ($U_0 ds$) upon the magnitude while deriving source parameters of intermediate magnitude shocks in the California-Nevada region. However, with the advent of high-gain long-period seismograph systems (Pomeroy et al., 1969) it became possible to observe and measure amplitudes of crustal waves from events of relatively low magnitude ($M_s \geq 3\ 1/2$) at epicentral distances as high as 1600 km. In the present study we intend to take advantage of such readings made at the Adolpho Bloch Geophysical Observatory at Eilat.

2. SENSORS, DATA AND COMPUTATIONAL SCHEME

Lists of events and signals used in our analysis are given in Tables 1-3. Three kinds of data are involved: (1) recordings made during 1968-1974 at the Eilat observatory,

(2) records of the July 11, 1927 earthquake at stations listed in Table 3.

The Eilat seismic station (29.3°N, 34.6°E) is located in the Amram massif, a large block of Precambrian granite-porphyry, unconformably overlain by Precambrian lava flows and associated tuffs and agglomerates. The rms background noise level in the band 0.1-1 sec (summer) is 2-5 mμ. Short period microseisms (6 sec) are uniformly small year around. Long-period noise spectrum, uncorrected for instrumental response, is flat. During 1968-1974 there were 16 seismometers in simultaneous operation: 3 WWSSN short-period, 2 WWSS long-period, 3 HGLP - high, 3 HGLP - low, 2 Benioff-major quartz-tube strainmeters and 2 long-baseline mercury tiltmeters. The magnification curves of all

instruments used in this paper are shown in Fig. 3. It comprises three generations of seismographs whose magnification at T = 100 sec range over five orders of magnitude.

Our method of data reduction and analysis is based on a merger of all known seismological techniques which up to now were dealtwith separately. Up to the present time most studies of crustal structure were done by the following 'source free' methods:

(1) Inversion of Love or Rayleigh wave dispersion data.

(2) Inversion of travel-time or $dT/d\Delta$ data (mostly from surface explosions).

Ignoring amplitude data, these methods are unable ab initio to supply data on tectonics, slip rate, and the unelastic properties of the crust. The method suggested by us treats the elastic and unelastic structure of the crust together with the tectonics of the area. We basically utilize the entire seismogram at each station to invert the eight-fold entity space:

(1) Initial P-wave motion.

(2) Travel-times of various P and S phases.

(3) P and S wave-forms.

(4) Radiation-patterns of Love and Rayleigh waves.

(5) Amplitude spectra of Love and Rayleigh waves.

(6) Dispersion of Love and Rayleigh waves.

(7) Attenuation spectra of Love and Rayleigh waves.

(8) Poisson-ratio depth-profile.

The computer programs needed for the indicated inversion methods are as follows:

(1) The Harkrider-Haskell dispersion and transfer-functions complex program for dislocation sources in multilayered elastic media.

(2) Powell's inversion scheme for surface wave dispersion and body-wave travel-times.

(3) Wickens-Hodgson fault-plane solution search.

(4) Calculation of theoretical spectrum for any given finite dislocation with arbitrary orientation and depth, coupled to a search program (Powell, 1970) δ(dip), λ (slip), ϕ_0 (fault azimuth) and h (depth).

(5) Radiation-pattern inversion scheme.

(6) Synthesis of Love and Rayleigh wave-forms over finite frequency range for dislocation sources in a multilayered inelastic half-space.

(7) The Ben Menahem-Vered program for exact synthesis of P and S wave groups according to Generalized Multilayered Ray Theory (GMRT) for dislocation sources of arbitrary orientation and depth. These are basically most of the numerical algorithms that seismologists have accumulated during the computer era. A schematic flow chart is given in Fig. 4 and is self explanatory.

Forty-seven local and regional earthquakes where then subjected, some in part and some in full, to the operational scheme sketched in Fig. 4. The results are discussed in the next section.

3. NEAR-EAST AVERAGE CRUSTAL STRUCTURE

Niazi (1968) obtained a two-layered crustal model of the central Arabian peninsula (H = 35 km) by matching observed phase and group velocities of Rayleigh waves in the period range 20 - 75 sec with a set of theoretical curves.

Goudardi et al. (1970) obtained a crustal thickenss of 39 km at Shiraz, using travel-times of crustal phases. Akasheh (1972, 1972a) studied the thickness of the Iranian plateau from travel times of P_n waves. He finds an average subcrustal P velocity of 8.13 km/sec and a crustal thickness that varies from 55 $\pm$ 7 km in central, western and northern Iran and a lower value of 49 $\pm$ 6 in South Iran. These authors consider it as evidence supporting the hypothesis that the Arabian plate shifted away from the Red Sea towards

north-east and dips down in south Iran.

The crustal structure of the region bounded from the south by the Red Sea, from the north by the Taurus mountains, from the west by the Mediteranean Sea and from the east by the Zagros mountains - was never before attempted. The structure of the buffer zone, which is compressed and sheared due to relative plate motion from the south to the north and north-east (Ben-Menahem and Aboodi, 1970), must reflect in some manner its geologic as well as its tectonic history. Because of the limited size of this region, it is essential to consider seismic signals that originated and were recorded in it. Moreover, since earthquakes in the Levant are mostly of small magnitudes, ultra high-gain seismographs are needed to monitor readable surface waves from events in the magnitude range 3 1/2 - 5.

This was not feasible prior to the establishment of the Eilat Observatory in 1968. Since then, high quality data of 19 events that occurred within 853 km from Eilat along the Levant fracture zone, were accumulated. In addition, the Eilat seismograms of 23 events occurring on the western margins of the Zagros thrust zone were also used to derive the structure east of the rift valley. The data were supplemented by reading from the KSARA Observatory bulletins. Wave paths and epicenters are shown in Fig. 5. Boundaries of the various geological provinces were drawn according to Amiran (1970). The relevant data concerning the 42 local and regional earthquakes in the magnitude range 3 1/2 - 5 1/2 used in the analysis is given in Tables 1 and 2. Forty-two Love and Rayleigh waveforms from which group-velocities were calculated are exhibited in Figs. 6-20. Most of these signals were recorded at Eilat on Long-period and ultra-long period seismographs during 1968-1974. The structural parameters were obtained from:

(1) Simultaneous inversion of Love and Rayleigh waves in the period range 7-50 sec.

(2) Observed travel-times of crustal reflections and refractions (P_n, S_n, P_IP, S_IS, P_MP, S_MS) which were identified with the aid of theoretical seismograms.

(3) Synthesis of body and surface-wave phases and their match with the observed isolated signals.

The inversion of the dispersion data was done with the aid of Powell's (1970) hybrid method. It is essentially a minimization of the sum squared of the difference between observed and theoretical group velocities. The method of operation is such that one begins the iterative process with an initial 'guess-model'. The parameters of this model are then varied automatically until a preassigned tolerance criterion is met. Since the final result depends strongly on the first guess, the 'guess-model' input-data must be carefully chosen. The best available model in the literature is that of Niazi (1968). However, the topmost layer in his model is a rather thin layer of very loose material that is inappropriate for the path of waves under consideration. We have therefore replaced it by a thicker layer of more consolidated materials (henceforth named modified Niazi model). The overall crustal thickness was preserved by appropriately reducing the thickness of the second layer in his model.

The inversion scheme yielded two distinct models. The first, called EILAT-EAST is based upon dispersion data of surface waves recorded at Eilat from earthquake sources north and north-east of the Persian Gulf (1-29 in Fig. 5). Inversion of Rayleigh and Love waves were carried out separately. Both sub-models are in very good agreement with the observations as well as with each other. The second model, called EILAT-NORTH is based on dispersion of surface waves from earthquake sources along the Jordan rift valley and its northern extension towards the eastern margins of the Taurus mountains.

Again, a separate inversion of Love and Rayleigh waves was performed.

The model based on Love-wave dispersion was determined by fewer observations.

The observed data clearly shows that both Love and Rayleigh group velocities in a northerly direction relative to Eilat are consistently higher than the corresponding group velocities in the easterly direction. We believe that this difference is due to higher upper crustal mean velocities in the northerly direction than in the easterly direction. Both observed and calculated velocities are exhibited in Figures 21 and 22. The resulting layered model is given in Table 4, where the values of the Poisson ratio for each layer were also calculated. Since the longest wavelength in our analysis (ca 200 km) did effectively sample only a depth of some 100 km, no effort was made to obtain structural parameters of deeper layers. The sub-crustal structure (including the upper mantle low velocity layer) must be probed with surface wave periods up to 200 sec, which were not available to us in the present analysis.

A study of Table 4 reveals the following features:

(a) A distinct Moho discontinuity with average crustal thickness of 35 km. In view of complementary results by other seismologists, it seems that the crust gradually narrows towards Eilat, both from the east (some 50 km in the Iranian plateau, Akasheh, 1972, 1972a; Goudarzi et al., 1970) and from the north (some 40 km in Turkey). Thus, the crustal thickness in the Levant is a mean between the eastern Mediterranean crust (ca 23 km, Papazachos et al., 1966; Payo, 1967, 1969) and the continental Asian crust (ca 50 km).

(b) Crustal shear velocities in Sinai and the Levant fracture zone (27° - 37°N) are significantly higher than the corresponding velocities in the eastern section Eilat-Zagros foothills. This partly reflects the influence of the deep marine sediments east of the Persian gulf (Fig. 5, Amiran, 1970).

The average shear velocity in the Eilat-north section is 3.51 km/sec, in agreement with previous independent results of Ben-Menahem and Aboodi (1971).

(c) All models share an extremely low value 0.205 - 0.188 for the Poisson ratio in the lower crust ($15 < h < 35$ km). Similar results were obtained by Papazachos et al. (1966) for south-eastern Europe and the eastern Mediterranean.

On the basis of the models given in Table 4 we have then derived theoretical travel-time curves for various phases and source-depths in the crust. These are plotted as solid lines in Figures 23a - 23f. Data were then collected from the EIL, JER and HLW readings and seismograms (Tables 1-3, Fig. 6-26). In addition, the bulletins of ISC, BCIS, ISS and KSA (Plassard and Kokoj, 1962, 1973) were used. The excellent fit of the observation to the theoretical predictions (Figs. 23a - 23f) confirms the results obtained via the dispersion of intermediate-period surface waves. Finally, as a second independent check, we have calculated by the GMRT method (Vered and Ben-Menahem, 1974) the P, S and Rayleigh waveforms due to an earthquake with known source parameters (Vered et al., 1975) in Iran, east of the Persian Gulf (Fig. 5). Fig. 27 shows the good fit.

In accord with our planned computational scheme (Fig. 4) we proceeded next to compute the surface wave transfer functions needed for the pending source studies. The results are given in Figs. 28-30 for the EILAT-NORTH earth model over the period range 5 - 60 s and source-depth ranges 0 - 35 km. The functions have already been divided by the angular frequency ω to accommodate for a step-function time-dependence suitable for earthquake dislocations in the mentioned period range.

4. SEISMICITY AND DISLOCATION CHARACTERISTICS

Having a fair knowledge of the average crustal structure we are now ready to tackle our chief objectives, namely: locating the active faults, evaluating their source parameters and finally, discovering the role played by them within the framework of global plate tectonics. With our limited available data we certainly could not hope to unveil every fault in the area. We were lucky however to have detected those segments of seismic activity which are vital to the understanding of the tectonic trends in the junction zone. These belong to four fracture systems and will be discussed below, starting from the Jordan rift valley, in a counterclockwise order.

(a) The Jordan Rift Zone and the Bikåa

The Jordan rift zone, including the Dead Sea is one of the most prominent morphological features in the entire Middle East. The elongated depression of the rift, bounded locally by normally faulted blocks on either side, is the trough for the Jordan River, which flows into the land-locked Dead Sea. This river was the life line of inumerable civilizations, who relied on its waters to revive the surrounding harsh desert. It is not surprising therefore that it is here at the entrance of the river into the Dead Sea where the oldest city known to men - Jericho - is located.

The most apparently impressive structural feature of the Dead Sea region is the predominance of normal faulting along the steep rims of the elongated valley of the sea as well as the Jordan River to the north. For this reason it was generally thought that the Levant fracture zone, extending from the Red Sea, through the Arava, Jordan valley and the Bikåa into eastern Turkey is part of a compressive or tensile force system. Because it is often much more difficult to notice horizontal motion along faults, early hypotheses that the Levant fracture zone (including, in particular, the Arava, the

Dead Sea and Jordan valley rifts) are in fact associated with important strike slip motion, were hotly rejected (e.g., Picard, 1967). But as geological investigations intensified, and detailed and improved observations were made, more and more evidence indicated that past horizontal motion with large offsets took place along this fracture zone. The most obviously relevant feature is the offset, at the entrance to the Gulf of Eilat, of the Arabian coast relative to Sinai by about 110 km. Dubertret (1932), Quennell (1956) and Freund (1965) have suggested on the basis of stratigraphic and structural evidence that the same shift can be found further north on land. Furthermore, Freund et al. (1968) have traced this shift for stratigraphic units of various ages, showing the progressive increase of total displacement with time. Zak et al. (1966) discovered very young stream offsets in the southern Arava near Eilat, which indicate horizontal strike slip motion along the local segment of the Levant fracture zone. The estimates of the average rate of slip varies from .65 cm/y (Freund et al., 1968) to 1.0 cm/y for the past 3-4 million years (Girdler, 1958). Motion here is therefore an order of magnitude smaller than for example along the San Andreas fault, in agreement with the global pattern of plate tectonics.

In spite of the mounting evidence in favor of the transform fault interpretation and large horizontal motion, seismological evidence is remarkably lacking. Whereas seismic activity is much less frequent than say along the San Andreas fault system, the surrounding regions nevertheless have experienced many destructive earthquakes, recorded over human history (Appendix A). Garfunkel (personal communication) identified the faint trace of an

active fault striking 11° east of north. In the field the fault trace can be recognized by disturbances in the flat-lying sediments of the Dead Sea basin. Furthermore, the fault trace is accompanied by several springs and disturbances of the drainage system. It appears as a sharp boundary between local badlands on the west and flat-lying beds to the east, between Jericho and the Dead Sea segment. Further north the fault causes, probably through drainage effects, pockets of arable land in which we find now small fruit orchards.

The fault apparently coincides also with the remarkably straight boundary between the Lisan formation and the recent Alluvium, which outcrops for several miles north of the Dead Sea.

The fault trace is quite clearly identifiable on air photos. It emerges from the northern end of the Dead Sea near the Kalia hotel, and forms a straight line through a series of small ridges. Further north it is marked by vegetation and changes in the drainage system. The trace in the photos is lost north of the Allenby bridge, as it approaches the Jordan river. There are also some faint indications, in the air photos, of short parallel fault strands to the east.

Dr. Brawer (personal communication) visited the Jericho-Allenby bridge area the day following the 1927 earthquake, because of rumors about peculiar occurences there. He reports a ground crack across the Jericho-Jordan monasteries road, running approximately from south to north and located about 1/2 - 1 km west of the banks of the Jordan flood plain. A photograph taken by an anonymous visitor from the American colony in Jerusalem some time after the earthquake shows a ground crack near the monastery of John the Baptist (Fig. 31). Whether these are two separate cracks or one is not clear, but both lie within a short distance east of the observed fault trace as shown in

Figure 32.

This site is apparently the pulse-beat of the seismic activity of the rift valley in the last three thousand years. According to tradition, it is there that the Israelites crossed the Jordan and there that Jesus was baptized by John the Baptist. The monastery was built for the first time in the fourth century A.D. and is the lowest monastery in the world (-356 m, Vilnai, 1968). It was ruined again and again by every major earthquake in the area. Tristram (1865) visited it on January 6, 1865 and found it completely in ruins. It was then rebuilt and heavily damaged again by the 1927 earthquake.

To the north, the fault trace can be inferred across the Jordan river by an escarpment which consists of upturned Neogene and Quaternary sediments and volcanics. The line then can be traced through two straight dry creek sections. We have also identified two possible small stream offsets, in the neighborhood of the town of Damia, Jordan. This is the area in which Braslawksi (1938) reports a mud slide into the river, following the 1927 earthquake. As shown in Figure 32, the instrumentally determined epicenter of this earthquake (ISS) falls nearby as well. The fault probably terminates here, and a new strand at the west side of the valley accommodates the motion.

In the Dead Sea to the south, the fault trace is more difficult to determine. It is clearly not the spectacular, albeit tectonically unimportant series of en-echelon steep normal faults, which form the western cliffs over the Dead Sea basin. Brawer (1928) Blankenhorn (1927) and Shalem (1956) reported a tidal wave with an amplitude of 1 meter on the northern shore of the Dead Sea at the time of the occurrence of the earthquake. In most liklihood, the fault trace can be identified by the floor topography, where the steep wall abruptly flattens. The bathymetry shows that this feature coincides

with the fault trace as it enters the sea in the north. Furthermore, the 1970 Ein-Gedi earthquake epicenter (see below) lies in the middle of the sea, practically on this inferred fault trace. The fault apparently terminates somewhere near the Lisan protrusion, and the motion is accommodated probably by the Arava strand to the east (Freund, 1965).

However, these seismic data and records have not successfully been combined to yield a clear picture of the earthquake source region. Various investigators proposed a multitude of source areas, based on destruction in various towns in the land. Furthermore, no clear relation has been established between the most important tectonic fault system in the area - the Levant fracture zone - and the seismic activity, recorded for about 4 thousand years.

It is reasonable to assume that all the historical and instrumental information on seismic activity and associated damage, as well as the tectonic and morphological data,must be explainable by a simple fault system, similar to known cases elsewhere. Furthermore, the activity must be related in a simple way to the most active element of global tectonics - the Jordan rift zone.

The geophysical problem is therefore to identify the seismically active fault, which is the source for many destructive earthquakes in the region, determine its orientation and obtain the direction of motion on it. Finally, we must find the relations between this fault and the geological and morphological features of the Jordan rift zone as part of the Levant fracture zone.

To meet these questions, we have studied the seismograms of six earthquakes whose epicenters are located on the rift zone. These are listed as no.'s 45, 33, 34, 37, 38 and 40 in Table 2. The corresponding seismograms are shown in Figures 10 - 15, 33 - 36. The strongest of these events, and

in fact, the most severe earthquake in the land of Israel since 1834, occurred on July 11, 1927. The ISS placed the epicenter at 32.0°N 35.5°E (ISS 1927, p. 247). The accurate macroscopic evidence of Brawer (1928), based on his personal experience and investigations, not only verify the location of this epicenter, but also substantiate a total fault length of some 40 km. This, as we shall soon see, agrees with our directivity length of 45 km. However, the ISS time of origin (15 03 55) is incorrect as it rendered high positive O-C residuals at near stations and also did not give the right arrival times of P waves at VIE, COP, UCC and DBN. This was mainly due to incorrect identification of crustal and subcrustal body phases at KSA and HLW. Solving our travel-time equations for body wave arrivals at these stations, the origin time t_0 = 13 04 07 was obtained, which indeed reduced the residuals to a reasonable minimum. Karnik (1969, 1971) for an unknown reason, listed the earthquakes once with the ISS origin time and again with 13 04 07, as found by us. He assigned to it a normal depth and M = 6. Aftershocks with magnitudes above 4.0 were listed by KSA and ISS and were shown in Figure 32. Seismograms of the main shock are shown in Figs. 33-35. Note the clear P phase (ptt ground motion 12μ at 2 sec) and the conspicuous SS phase (ptt ground motion 50μ at 13 sec) which are seen on the EW VIE Wiechert.

Surface-wave signals recorded at Copenhagen, De-bilt, Capetown, Vienna and Uccle were identified by their group velocities and then digitized and subjected to Fourier analysis. The observed spectra were then corrected for instrumental response, attenuation (Fig. 36) and geometrical spread. The resulting entities were then plotted against the period and compared with the corresponding theoretical expressions (eq's 1-2). A best fit with the observa-

tions at five stations yielded the source parameters listed in Table 5. The spectral ground displacements are shown in Figure 37.

It is seen that the directivity effect is very pronounced. The spectrums of four European stations show a hole around 30 sec, where the backward Rayleigh radiation field has its first destructive interference order.

The spectra reveal therefore that the source was moving southward toward Capetown. For that reason, the forward Love radiation field should not vanish, per theory, anywhere in the period range 10 - 50 sec. This is indeed what we see in Figure 37. Unfortunately, the EW seismogram at CTO was not available to us. Nevertheless, the Love wave there was so strong that its NS amplitude (even at that relatively large distance and in a quite unfavorable inverse azimuth), was sufficiently high. On the other hand we were quite fortunate to have the seismograms of VIE, COP, DBN and UCC, since these stations were located on a node of the Love radiation-pattern and consequently their horizontal recordings are almost free from interference of Love and Rayleigh waves. In Uppsala however, interference between the shorter Love waves and the longer Rayleigh waves prevented us from using the data. The equalization of the observed and theoretical amplitudes yielded an average potency of 18,000 cmxkm^2, (COP 22,000; VIE 20,000; UCC 17,500; DBN 14,000; CTO 18,000) an average fault-length of 45 km and a vertical extent of some 10 km. The average amount of slip was, therefore estimated as 40 $\pm$ 10 cm. Figure 38 shows the realm of activity of the Dead Sea fault. Since 1927 no

shocks of comparable magnitudes recurred along the Dead Sea fault. Smaller events, though, have been continuously recorded by KSA and JER, but it was not until the establishment of the Adolpho Bloch Geophysical Observatory at Eilat in 1968, that high-gain long-period recordings, necessary for the study of small-magnitude events, became available. Thus, the first earthquake that could properly be studied occurred on Oct. 8, 1970. It was preceeded by a smaller foreshock, 10 hours earlier. Seismograms of the WWNSS and the LP seismograms at EIL are shown in Figures 10-12, 39 and 40. The amplitude equalization results at EIL, HLW SHI and AAE are shown in Figures 41 and 42, and Table 5. Figure 43 shows the observed vs. calculated radiation pattern for both Love and Rayleigh waves from the Oct. 8, 1970 event. Indeed, the polar diagram at 25 sec is in full accord with the inversion of the spectral amplitude functions. The attenuation curves (Fig. 36) are based on the data of Tsai and Aki (1969), Aki and Tsai (1972) and Ben-Menahem (1975) but exhibit stronger dissipation at the shorter and longer period over Mid-Eastern paths. All the observed data in Figure 43 were equalized to the distance of EIL to the respective source. Throughout this paper directivity effects were neglected at periods above 10 sec. for all events with $M_s \leq 5.1$.

Initial motions of P and SH signals at EIL, JER and HLW (Figs. 10-12, 26, 33, 40) from the Dead Sea region earthquakes are in full agreement with the spectral results. Consider for example Fig. 40, where the initial motions at JER are clearly visible on all three components, indicating a dilatation from the south-east (Fig. 31). The P and SH motion at Eilat (Figs. 10, 12) agree with this polarity.

The three shocks discussed so far delineate a major

fault which runs from the Damia bridge (Fig. 32) down to the middle of the Dead Sea, opposite En-Gedi, with an overall length of some 75 km. This fault, when slipping along its entire length, may produce an earthquake of magnitude 7 - 7 1/4. While during 1927 - 1930 the activity centered on its northern tip, it seems that since 1968 or thereabouts the activity shifted toward its southern tip at 31.45°N, 35.49°E.

To examine the tectonics of the rift zone north of the Dead Sea we have analyzed the seismograms of three events. The earthquakes of Sept. 7, 1971 and Nov. 8, 1971 were well recorded on the EIL tiltmeters and HGLP. The epicenters were located with the aid of short-period P arrivals to EIL, JER and KSA. One of these events was reported by the ISC. Love waves show up very clearly with a typical normally dispersed wave-train (Fig. 15). Rayleigh waves are however absent, as expected from a strike-slip motion in the general NS direction. An equalized spectrum at Eilat is shown in Fig. 44 and the source parameters are given in Table 5. The epicenter of the third event (Sept. 2, 1973) was located right in the middle of the Sea of Galilee. Seismograms are exhibited in Figures 13 and 44 and the equalized spectra at EIL and HLW in Figure 45. We believe that our location is quite accurate because at that time we were operating a small network of portable vertical short-period seismometers. In addition to the recordings at EIL (iP 04 02 18.5), JER (iP 04 01 48.5), KSA (iP 04 01 39) and HLW (iP 04 02 39) we had the P arrivals at Kibutz Alonim(32°43'31"N, 35°08'10"E, ip 04 01 36), and Kibutz Afik (32°46'30"N, 35°41'05"E, iP 04 01 30), just 11 km east of the epicenter. Again, the amplitude ratio (Love/Rayleigh) at T = 15 sec at Eilat was about 10:1, suggesting a strike-slip motion at the source. We nored that on the LP recordings at HLW, Love arrivals were missing on both horizontal components,

indicating a nodal direction for Love waves. Indeed, the azimuth of HLW relative to a fault striking 7° west of south is exactly 45°, which is a Love-wave node for a strike-slip dislocation.

A relatively high (Love/Rayleigh) amplitude ratio at SHI (located almost at right angle to the fault), supports a source model with dominant strike-slip compnent.

(b) Palmyra Chain

The study of this zone is done here via two earthquakes recorded at Eilat during 1970-1974. A literature search has shown that very little is known about the geology of the area, let alone its tectonics. Historical seismicity is briefly discussed in Appendix A-III. Data concerning the earthquakes under study is given in Table 2. Results are listed in Table 5. Calculated vs. observed spectra are given in Fig. 46 and the corresponding waveforms are shown in Figures 16-17. We note the isolated R_{21} mode arriving just ahead of the fundamental R_{11} mode, with a group velocity of 3.45 km/sec at 5 sec and 3.3 km/sec at 7 sec as compared to 2.58 km/sec of R_{11} at the same period. The R_{21} mode was positively identified by the match of its observed group velocities to those calculated for the Eilat-north crustal structure (Table 4). We took advantage of these isolated arrivals to derive the source's mean depth from the spectral ratios R_{11}/R_{21} (Fig. 17). With the source parameters as determined from the inversion of the Love and Rayleigh spectra, a focal depth of 32-36 km was obtained, in complete agreement with the determinations of USCGS (33 km) and ISC (34 ± 6 km). This determination provided therefore an independent check both on our crustal structure and dislocation elements derived by amplitude equalization. We have chosen

the direction of the strike to coincide with major fault traces (N50 - 70E), observed in ERTS photos, which are parallel to the general trend of the Palmyra mountain chain. With this choice, we find strong left lateral strike motion, accompanied with reversed, not normal, dip slip. The relatively shallow dip also indicates thrust type motion for both events.

(c) Amanus-Taurus Mountains

The tectonics of the northern edge of the junction has previously been summarized by Nowroozi (1971, 1972), It is based mainly on the alignment of epicenters along the margins of the Zagros-Taurus thrust and a few fault plane solutions (Canitez and Ucer, 1967; Shirokova, 1967). The Amanus-Taurus junction is the meeting area of the NS trending Syrian-African rift with the EW trend of the Taurus mountains. Historical (Appendix A-II, Plassard and Kokoj, 1962) records indeed indicate continuous seismic activity near Antioch-Iscanderun. To estimate the present rate of slip along the northern edge of our plate, we have studied the long-period Eilat records of the July 11, 1971 earthquake. This was supplemented by a reexamination of the fault plane solution of the April 8, 1951 earthquake (Tables 1,2,5). Time-series are shown in Figure 9. Spectra are shown in Figure 45 and fault plane solutions in Figure 49. Our results for the April 8, 1951 event agrees with those of Shirokova (1967). The similar solution of Canitez and Ucer (1967, $\delta = 68°$, $\lambda = 164°$, strike = N295°E) is within the limits of error. Initial motions were read from the ISS, USCGS and ISC reports. Clearly, a unique choice of the fault plane cannot be made from either first motion data or from the inversion of the spectral amplitudes. In this case, however, we choose the EW strike solution (Table 5) parallel to the tectonic thrust line.

(d) Off-Shore Faulting, Tsunamis

Historical earthquakes off-coast the eastern Mediterranean are listed in Appendix A-II. Sieberg's isoseismals of some of the major events were already shown in Figure 1. The data, important as it is, does not tell us the location of the faults, nor does it render useful information concerning the orientation and slip rates on these faults. The Ksara, Lebanon, map of epicenters for 1961-1970 shows however a clear alignment of marine epicenters in three parallel segments stretching from Tartous to Tyre (Fig. 50). These are perhaps some of the faults responsible for the three score or so tsunamis that wrecked the Levant coastal cities repeatedly since 600 B.C. (Appendix A-II).

Fortunately for the inhabitants of these cities, but unfortuantely for seismologists, the submarine activity in this region lessened considerably during the past century, and tsunamigenic earthquakes are hard to come by. We were forced therefore to settle with two "harmless" events of magnitude 4.7 - 4.8, which we believe, bear the characteristic features of the zonal tectonics. These are the events of March 26, 1968 and April 6, 1971, whose epicenters are only 60 km apart.

Waveforms are shown in Figures 14, 24, 44 and 50. The corresponding amplitude spectra are exhibited in Figures 52-54. Initial motions are shown in Figure 49 (data from WWNSS, LP records. Supplemented with ISS, USCGS, BCIS and ISC reports) and radiation patterns in Figure 43. Pertinent data concerning these events are given in Table 2. We note from Figure 51 that although the wave-paths and the magnitudes of the two events are almost the same, the ratio R/L at 20 sec as recorded in SHI, east of the epicenters, differ considerably. This is found to be due to different strikes of the two dislocations. Table 5 lists the source parameters. The direction of the strike

of these faults is uncertain. Freund (1965) suggested that a series of right lateral geological strike slip faults, trending NE on land in Lebanon, are participating actively in the deformation of the crust. This pattern is consistent with one set of solutions (λ = 199°, δ = 76°, N144°E). We prefered however to choose the alternate set of solutions with N-NW strike directions. These solutions yield normal faulting as well as left lateral strike slip, indicating subsidence of the sea side - as implied by historical evidence (Appendix A-II). Both solutions dip towards the east and have a dominant strike-slip component.

Both earthquakes have a dip-component ($u_o \sin \lambda \sin \delta$) of about 50 percent ($1/2\ u_0$) which is highly tsunamigenic for magnitudes above 6.

Striem and Milch (1975) have argued in favor of the possibility that historical tsunamis at the coasts of Israel and the Levant may have been caused by slumping on the continental slope. Based on data of actual submarine scars, they found that the slumping of a mass 6 km long, 2 km wide and about 50 m deep would cause a formation of a shock-induced solitary wave of about 10 m in height at the edge of the continental slope. This, according to their calculations, would cause the accompanying draw-down of the sea level at the coast, to last about 1/2 to 1 1/2 hours, and lay the sea floor bare for a distance of about 1/2 to 1 1/2 km, in agreement with some historical descriptions.

(e) The Sinai Triple Junction and its NW Extension

While the motion of the African plate relative to the Arabian plate has been established experimentally (Ben-Menahem and Aboodi, 1971), the role of the Sinai Peninsula in the regional tectonics is still unclear. Geologists differ widely in their opinions, mainly due to the lack of a dominant trend of visible faulting in the Sinai-Africa border zone. On the other hand, the seismic activity in the past two decades north of the 28° parallel in this area was such that no clear demarcation line of epicenters could be drawn.

Under these conditions, especially in the lack of geological guidelines, one is left at present with a single choice, namely, the study of the seismic radiation field from a group of selected local events of a magnitude that is high enough to represent dominating tectonic features.

Historical earthquakes in upper Egypt are listed in Appendix A-IV. Since the establishment of modern seismographs in the early thirties, only very few local events were adequately recorded outside Egypt. A literature search revealed available initial-motion listings for two earthquakes only; Sept. 12, 1955 and Jan. 30, 1951 (Schaffner, 1959; Shirokova, 1967; Wickens and Hodgson, 1967; Canitez and Ucer, 1967; McKenzie, 1972). The establishement of the ultra long-period seismograph at the Eilat Adolpho Bloch Geophysical Observatory, in 1968, opened for the first time the possibility for a serious study of the region's tectonics. Since then, two earthquakes with magnitudes above 4 3/4,

originating within a radius of 600 km and inverse azimuths range 200° - 325°, were recorded at Eilat with sufficient power over a wide spectral band. One of these, dated March 31, 1969 (M = 6 1/2 - 6 3/4) was already studied by us (Ben-Menahem and Aboodi, 1971). The second earthquake of April 29, 1974, was of smaller magnitude. The shock was felt strongly in the Suez, Egypt and southern Israel and was recorded by LASA (Δ = 94.27°, AZ = 332.5°). Eilat seismograms are shown in Figures 19, 20 and 25. Amplitude spectra are given in Figure 55 and an initial motion solution (based on readings of the stations HLW, EIL, IST, KDZ, JOS, PSZ, MOX, WLS, BNG, CLK, KRR, CIR, ALE, FFC) is exhibited in Figure 49. Love and Rayleigh waves recorded at the WWNSS of UME and NAI were also used. Pertinent data and source parameters are given in Tables 2 and 5. According to Gergawi and Khashab (1968) there are two active narrow seismic belts in northern Egypt and Sinai that meet at (31.3°E, 30°N). The weaker belt is oriented about N50°E and the stronger is oriented N10°W north of the crossover point. A north-west faulting (called Erythrean or African) cuts through the stable shelf of Egypt. The trend NW-SE seems to be old. Faults of similar trends are traced all over the country. It is assumed that the river Nile entered the present Delta region after its tectonic formations not later than upper-Oligocene times. The delta collapse took place below sea level, prior to the regression of the sea. The delta unit is a triangle corresponding to the Sinai, only with the difference that

the Sinai is elevated (its boundary faults dipping away from the unit) while the delta structure is low-land (border faults dipping towards the unit). The choice of the correct fault plane solution is in this case more difficult than in the other geological provinces discussed so far. We shall therefore start with a summary of the various existing tectonic theories for this region and judge them in the light of our findings.

Although the nature of the motions on Arava - Dead Sea fault, and the opening of the Red Sea are reasonably understood in a general way, the details of the motion are not yet clear. One difficulty arises upon comparison of the total opening of the Red Sea - about 190 km (Girdler, 1965), and the total slip on the Arava-Dead Sea fault which is only about 110 km (Freund, 1965). How is the missing motion of 80 km accommodated? The second difficulty is the role of the Gulf of Suez in the tectonics of the region. Many investigators ignored the Gulf of Suez, by assigning the entire slip between the Arabian and African plates to the opening of the Red Sea and the approximate transform fault nature of the Arava-Dead Sea fault (e.g., Nowroozi, 1972; Girdler, 1965). This solution fails, as mentioned, to explain the discrepancy of 80 km.

Picard (1966) suggested that the Gulf of Suez is the expression of Graben tectonics - dominated by vertical tectonic movements. McKenzie et al. (1970) combined Picard's notion with the opening of the gulf similar in sense with the opening of the Red Sea, although by a smaller amount. In this way they argue, the missing slip along the Arava may be taken up. They point out however that a significant discrepancy remains, in that the Gulf of Suez can accommodate only 50 or 60 km at most, leaving at least 20 or 30 kms unaccounted for. Youssef and Le Pichon (1973) suggested on the basis

of the geometry of the shore lines that the Gulf of Suez consists of WNW trending ridge segments and perpendicular transform faults with right lateral motion. Kenyon et al. (1975) proposed east west ridge segments, with short NNE trending left-lateral transform faults. Neev (1975), without mentioning the Gulf of Suez per se, proposes a tectonic line approximately perpendicular to the gulf with left lateral motion in a NE trend.

Freund (1965) suggested that the trend of folds in the Suez area implies some left lateral strike slip motion along the Gulf of Suez. Abdel Gawad (1969) proposed that this type of left lateral motion along the gulf could accommodate the entire difference between the total slip on the Arava-Dead Sea rift and the opening of the Red Sea.

The fault plane solutions obtained here for the Zagazig 1974 and the Alexandria 1955 earthquakes, in combination with the established solution for the March 31, 1969 Red Sea earthquake , provide tight constraints not only on the motion across the Gulf of Suez, but also upon the relative motion between the Arabian, Sinai, and African plates. These earthquakes have one common set of fault plane solutions with strikes N30-40W, steep dips to the NE, and a pronounced left lateral strike slip component of motion. Furthermore, the three events lie on a line which coincides with the average direction of their strikes, as shown in Figure 56 . The strong presence of the left lateral motion on the NW trending faults immediately excludes the models of Le Pichon (1973) and Youssef (1968) which require right lateral strike slip motion in this direction. The set of 3 dual solutions has strikes to the NE, with significant right-lateral strike-slip motion. Therefore, the models of Neev (1975) and Kenyon et al. (1975) which require left lateral slip along NE trending strike slip faults are both incompatible with the seismic data.

For all 4 events the possible fault plane solutions have a dominant strike-slip component. This implies that the model of McKenzie et al. (1970) for the opening motion of the Gulf of Suez is insufficient. Similarly, Picard's (1966) and McKenzie's (1970) motions of graben tectonics, requiring mainly normal faulting, find no support in the seismic results. The coherency of the motion obtained from the three events implies also that the Gulf of Suez is seismically active, although at a low rate, and cannot be ignored.

The results are in qualitative agreement with the suggestion of left-lateral strike-slip motion along a NW trending direction by Freund 1965) and Abdel Gawad (1969). Our proposed interpretation of the results is shown in Figure 56. The western corner of the Arabian plate, the intersection of the Gulf of Eilat and the Red Sea, moves relative to Africa, along the trend vector as obtained from the 1969 Red Sea earthquake (Ben-Menahem and Aboodi, 1971). This trend is not parallel to the Gulf of Eilat strike-slip fault, making an angle ϕ_2 with it. Thus only part of the motion appears as relative left lateral strike-slip movement u_1 between Arabia and Sinai, and the rest is taken up by a combination of left lateral slip u_2 and opening Δu along the Suez line, which makes an angle ϕ_1 with the trend vector of Arabia relative to Africa. Neglecting curvature, we find the geometrical ratio between the strike-slip motion along the Gulf of Suez u_2 and the Arava fault u_1

$$\frac{u_2}{u_1} = \frac{\sin\phi_2}{\sin\phi_1} \qquad (1)$$

and the ratio between the strike slip motion u_1 and the relative opening of the Red Sea u_A to the Gulf of Suez Δu at the triple junction

$$\frac{u_1}{u_A - \Delta u} = \frac{\sin \phi_1}{\sin(\phi_1 + \phi_2)} \qquad (2)$$

The sum $\phi_1 + \phi_2 \cong 45°$ is the angle between the Gulfs of Suez and Eilat. The angle ϕ_2 can be estimated in three ways: (1) directly from the trend of the seismic motion during the 1969 Red Sea earthquake, which yields (Ben-Menahem and Aboodi, 1971) $\phi_2 \approx 0° - 12°$; (2) from the direction of motion of the Arabian plate relative to the direction of the Arava-Dead Sea fault, which yields (McKenzie et al., 1970) $\phi_2 \cong 8° - 12°$; and (3) from equations (1) and (2), using the known total slips of the Red Sea and the Arava-Dead Sea fault. McKenzie (1970) suggested $u_0 = 190$ km, $u_1 = 110$ km and $\Delta u_0 \approx 60$ km. This yields $\phi_2 = 8°$, and left-lateral motion strike-slip/along the Gulf of Suez of 26 km. $\phi_2 = 8°$ is in good agreement with the other estimates. Thus if we add to McKenzie's solution for the Sinai junction problem, a left strike-slip motion of 26 km since Cretaceous time, the discrepancy between the opening of the Red Sea and the slip on the Arava fault are perfectly reconciled. Consequently, it appears that an opening of the Gulf of Suez of about 1/10 of the Red Sea since Cretaceious time, combined with left

lateral strike slip of about 1/4 the slip on the Arava fault, provides a good explanation for the tectonic movements associated with the triple junction of the Arabian, African and the so called Sinai plates. In particular, the model predicts a left lateral slip rate of 1 - 2 mm/y along the Gulf of Suez, given the 6 mm/y along the Arava-Dead Sea fault system (Freund et al., 1968).

In addition, we also notice that the Alexandria 1955 earthquake trend shows no dip slip (or even some thrust motion) on top of the large strike slip, whereas the Zagazig solution has a clear normal dip slip component. This could indicate a general anticlockwise rotation of the Sinai and Sinai-Arabia blocks relative to Africa. This rotation is possibly part of the overall relative rotation of the Arabian plate (McKenzie, 1970). The uncertainty in the Alexandria fault plane solution excludes quantitative evaluation of this effect, however.

5. GENERAL TECTONIC FEATURES

From the calculated crustal structure and fault plane solutions for the Afro-Eurasian junction, we obtain two general features. First, we analyse the state of the crust and second we study the tectonic motions which are currently taking place. We also estimate the seismic hazard zone for future events on the Dead Sea fault.

(a) Regional structure

(1) Surface wave magnitude vs. potency. Although relations of this kind

were previously investigated (Chinnery, 1969; Johnson and McEvilly, 1974) we had the unique opportunity of checking its validity from high quality data for a relatively small area.

A least square fit to the potency data yielded the result

$$\log_{10}[u_0(\text{cm})ds(\text{cm}^2)] = \alpha M_s + \beta \; ; \quad \alpha = 1.61 \pm 0.1 \quad ; \quad \beta = 4.01 \pm 0.2$$

$$3\ 1/2 \leq M_s \leq 6\ 1/2 \tag{3}$$

as compared to $\alpha = 1.27$, $\beta = 6.52$, and $\alpha = 1.16$, $\beta = 6.12$ obtained respectively by the above authors for the North American continent.

The seismic slip during the 1927 event was about 400 mm. The previous comparable event occurred in the same area in 1837 (Appendix A). This yields an average slip rate of about 3 mm/y . On the other hand, the slip rate estimated from plate tectonics and geologic offsets are 6-10 mm/y (Freund, 1965; Le Pichon, 1973). Furthermore, out of the 40 reported earthquakes during the 2000 years, 10-15 were comparable to the 1927 event. This also yields a slip rate of about 3 mm/yr. This evidence suggests that at least mm/y of aseismic slip must also take place on the Dead Sea fault. Further south, on the Arava fault, seismicity is lower and therefore aseismic slip is probably even greater.

(2) The state of the crust. Three features of the crustal structure in the area of study are of particular interest: (1) as in many other transform fault zones, seismicity is confined to the top 20 km of the crust, with the exception of the thrust events in Palmyra and the Taurus zone. Thus, unless thrusting occurs, the apparent brittle behavior of the crust terminates at a depth of 20 $\pm$ 5 km. (2) Poisson's ratio is unusually low at a depth

of roughly 20 $\pm$ 5 km, down to 0.18-0.20 from values of 0.25 - 0.27 just above or below this depth. Braile et al. (1974) found a shallow crustal low velocity zone in Nevada, with an abnormally high Poisson's ratio at depth of 10-15 km, a marked decrease below that depth, and a subsequent increase. However the values of their ratios were all markedly higher than obtained in this study. (3) As shown in Figure 36, both Love and Rayleigh waves Q have large peaks at about 25 seconds. The ratio of the inverse Q's, Q^{-1}, gives $Q_R^{-1}/Q_L^{-1} = 0.5 - 0.7$, where R and L denote Raleigh and Love waves respectively. Tsai and Aki (1969) obtained similar results, in which Q increases greatly towards the lower crust, and their experimental ratio $Q_R^{-1}/Q_L^{-1} = 0.6 - 0.7$. Mitchell (1973) found, from Rayleigh waves alone, that Q increases rapidly in the U.S. midcontinent area at a depth of approximately 20 km.

If we ignore anisotropy and scattering then the observed low ratio of Q_R^{-1}/Q_L^{-1} implies that Poisson's ratio must be small (see White, 1965, p. 102). Thus it appears that a minimum in Poisson's ratio with depth is consistant with the observed Q ratio. As suggested by Housley et al. (1974) the high, midcrustal Q values may be caused by the disappearance of water bearing cracks at that depth. Qualitatively, this implies also a reduction in Poisson's ratio (Nur, 1972; Spencer and Nur, 1975), and by definition, a drastic increase in effective confining pressure, as pore pressure is non-existant. This implies that the rock is subject to large confining pressure, and may be ductile here.

In a qualitative way we propose then that the crust contains cracks and pressurized water to a depth of roughly 20 km. Thus Q is low, Poisson's ratio is somewhat high, and rock is weak and brittle. At approximately 20 km depth, cracks and pore fluid disappear, the rock becomes ductile and does not produce an earthquake, Poisson's ratio decreases, and Q greatly

increases. The details of this model, which must include effects of pressure, temperature, porosity distribution, fluid properties and rock properties will be given in a separate paper.

(b) Tectonic movements

It has generally been assumed that the Levant fracture zone is dominantly a strike slip fault system, transforming the opening motion of the ridge-like Red Sea into the collision zone of the Alpine Mountain belt. As such, this zone is one of the three main transforms associated with continental collision on earth. Together with the Owen and Assam fracture zones, the Levant zone defines the boundaries between the three rigid plates - Africa, Arabia, and India - which collide with the Eurasian plate to produce the Alpine-Himalayan Mountain belt.

Unlike the Owen fracture zone, most of the Levant zone is well exposed on land, and unlike the Assam zone in Burma, it simply divides between two rigid plates - Arabia and Africa - which move approximately in the same direction but at different rates. Thus this zone provides insight into the way by which coherent, rigid plates transform into highly deformed, incoherent mountain belts.

The overall pattern of seismic deformation of the Afro-Eurasian junction associated with the Levant fracture zone, is shown in Figure 56 and Table 5. Whenever possible we chose the direction of seismic faulting to coincide with known prominent geologic faults such as in the Palmyra region, the Amanus-Taurus mountains, and the Dead Sea fault. Along the Gulf of Suez we chose the fault directions which are parallel with the Gulf, defining in this way a fault system trending through the Gulf into the Mediterranean Sea. The fault directions for the two events off the Coast of Lebanon were chosen to explain the occurrence of tsunamis and on the basis of similarity

with the known strike slip faults in northern Israel. The direction for the single event in the sea north of Sinai was chosen for its similarity with the Gulf of Suez events.

With these selections we recognize at once that the horizontal strike slip component of motion is left lateral everywhere - like the left-lateral motion along the Dead Sea fault itself. Aside from the main fault events, which are purely strike slip, all other events have a dip slip component. West of the Dead Sea transform the motion is invariably that of normal faulting - observed as we see for 6 events. On the east, the two Palmyra events have clear thrust motion components. This pattern, antisymmetric about the main fault, suggests a simple tectonic picture in which left lateral motion with compression occurs on the faster moving Arabia plate along NE trending faults and left lateral motion with tension takes place on NW trending branch faults on the slower moving Africa plate - including the Gulf of Suez and its extension. This picture is supported by available geologic evidence indicating normal faulting in the Gulf of Suez region, possibly including the tensile surface fractures in Ras Muhamed, at the southern tip of the Sinai peninsula. Furthermore, Freund (1970) has shown left lateral strike slip motion on several faults in northern Israel as well as overall north-south elongation.

A rough model gives a simple interpretation of the observed motions. As the Dead Sea transform leaves the Red Sea, the relative slip along it diffuses sideways into the array of branching faults. These faults are thus responsible for the breakage of the plate regions adjacent to the transform fault. As we approach the collision zone - the Amanus-Taurus mountains - less and less relative slip between Arabia to the east and

Africa to the west is accommodated by the main transform fault, as the cumulative slip on the branch faults is increasing. Figure 58 shows, in a schematic way, the nature of the motion associated with break-up of the plate boundaries. Point P, which was situated at the intersection of a NE branch fault with the main transform,has moved with time to Q with a component of motion parallel to the main fault, plus a component along the branch fault, which has itself moved northward as part of the Eastern Arabia plate. A point P' on the western plate has moved only to Q', as the Africa plate moves slower than the Arabia plate.

This interpretation predicts that the slip rate, or total slip along the main transform,decreases from south to north. If Arabia moves at an overall rate $\dot{u}_1$ and Africa at $\dot{u}_2$, then the relative slip rate between them is $\Delta\dot{u}_0 = \dot{u}_1 - \dot{u}_2$ at the Sinai triple junction. The slip rate on points further north such as $\Delta\dot{u}_n$,is then given roughly by

$$\Delta\dot{u}_n = \Delta\dot{u}_0 - \sum_{i=1}^{n} \Delta\dot{v}_i \cos \phi_i \qquad (4)$$

where $\dot{v}_i$ is the slip rate on branch fault i and ϕ_i is the angle between the branch fault and the main transform. The summation indicates the contributions of all the branch faults between the origin at the Red Sea to the point on the transform. By multiplying each side of equation 4 by time t, we obtain the relations between average total slips.

As shown earlier, the Gulf of Suez motion approximately explains the discrepancy between the slip rate (at the Red Sea) of $/\Delta\dot{u}_0 \cong 1.1$ cm/y between Arabia and Africa, and the estimated .65 cm/y along the Arava fault. Assuming that the faulting in northern Israel, Lebanon and Palmyra has

accommodated a total of approximately 30 km, we find that slip rate on the Bikåa fault should be only about .45 cm/y. This is qualitatively consistant with observed geologic offsets which also show smaller total displacement in the northern part of the Levant fracture zone.

Another major effect of this kind of breakup (besides reducing the slip rate along the transform fault) is to smear out the jump in collision rate $\dot{u}_D \equiv \dot{u}_1$ for the faster Arabia plate and $\dot{u}_A \equiv \dot{u}_2$ for the slower Africa plate. Thus the collision rate at points B and C in Figure 38 are approximately

$$\dot{u}_B = \dot{u}_A + \frac{1}{2} \Delta u_1 \quad \text{and} \quad \dot{u}_C = \dot{u}_D - \frac{1}{2} \Delta \dot{u}_1 \tag{5}$$

We estimate that the average collision rates in the Amanus-Taurus mountains is 3.3 - 3.7 cm/y, significantly less than the 4 cm/y for the Arabia-Zagros collision, and more than the 2.9 cm/y of the Africa-Europe collision (Le Pichon, 1973).

It should be pointed out here that the slip rates calculated from the repetition rate of earthquakes is not sufficiently accurate to test our model. However the comparative seismic activity is consistant with historical evidence (Appendix A). For example, there are only about 1/6 the number of events in the Suez region during the past 4000 years, as there were on the Dead Sea fault during that time.

In summary, the seismic and geologic evidence associated with the junction zone shows that this is the region in which the edges of the coherent Arabia and Africa plates break up in the neighborhood of their boundary as they approach the region of continental collision with the Eurasian plate. This breakup consists of gradual loss of coherency of the plate, and deterioration of its rigidity - as more and more deformation is taken up by branching faults. At the collision zone istelf - in the Amanus Taurus mountains -

the plates have lost of course their entire rigidity. It is noteworthy that the region of breakup extends away from the collision zone by a distance comparable to the length of the irregularities in the shape of the collision-induced mountain-belt of a few hundred kilometers.

Finally, we have identified the source fault for many of the biblical and historical earthquakes including the 1927 event, which have shaken Jerusalem, Nablus and Jericho for several millenia at a mean rate of two per century at magnitudes 5 - 7. The fault runs from Damia into the Dead Sea towards En Gedi. Figure 38 shows an outline of the predicted seismic hazard zone compared with the intensity data for the 1927 Jericho earthquake. This zone defines the most likely areas of future seismic risk associated with the Dead Sea fault.

6. CONCLUSIONS

We have investigated the crustal structure and tectonics of the Afro-Eurasian junction region from (1) observed body and surface signals that originated from earthquakes inside the region and were recorded within it; (2) geological and morphological data related to faulting activity; and (3) historical, including biblical and post biblical evidence for seismicity and seismic destruction as well as tsunamis. We have judiciously combined these data with the theory of seismic radiation from a finite size, moving dislocation source; inversion of surface wave data, the Wickens-Hodgson fault plane solution method, and theoretical models for surface and body wave radiation, together with models of plate tectonics, crustal physics and crustal deformation.

We find the following main crustal features: (1) A distinct Moho discontinuity with average crustal thickness of 35 km, which is intermediate

between 23 km for the eastern Mediterranean and 50 km for continental Asia. (2) Low values of Poisson's ratio of 0.18–0.21 at depths of 20 - 25 km; low Love (Q_L^{-1}) and Rayleigh (Q_R^{-1}) attenuation values around a 25 second period, with a low value of $Q_R^{-1}/Q_1^{-1} \approx 0.5 - 0.7$; and all events are shallow, usually less than 20 km deep. We suggest that the crust contains cracks and pressurized water to a depth of about 20 km. Thus Q is low, Poisson's ratio somewhat high, and rock is weak and brittle. At about 20 km depth, cracks and pore fluid disappear, the rock becomes ductile, Poisson's ratio decreases and Q greatly increases, and earthquake activity ceases. (3) Crustal shear velocities in Sinai and the Levant fracture zone are signifcantly higher than the corresponding velocities in the eastern Eilat-Zagros foothills.

By analyzing earthquakes since 1927 we find the following tectonic features:

(1) The seismic slip on the Dead Sea-Bikåa section of the Levant fracture zone is pure left lateral strike slip motion, in a direction coincident with the trend of the geological strike slip fault trace.

(2) We find that an opening of the Gulf of Suez of about 1/10 of the Red Sea since Cretaceous time, combined with left lateral strike slip of about 1/4 the slip on the Arava fault provides a good explanation for the tectonic movements associated with the triple junction of the Arabia, Africa and the so called Sinai plates. In particular we estimate a left lateral strike slip rate of 1-2 mm/y along the Gulf of Suez.

(3) Deformation is not confined to the fracture zone itself. With independent choice of the direction of faults, we obtain a pattern of branching faults, as shown in Figure 56. This pattern, antisymmetric about the main fault, yields a simple tectonic picture in which left lateral motion with compression occurs on the faster moving Arabia plate along NE trending

faults, and left lateral motion with tension takes place on NW trending branch faults on the slower moving Africa-Sinai plate. Consequently, as the Dead Sea transform fault leaves the Red Sea, the relative slip along it diffuses sideways into the branching faults. Thus in this region the edges of the Arabia and Africa plates break up and lose their coherency as they approach the Amanus-Taurus region of continental collision.

(4) Our interpretation implies that the Sinai region should not be considered a separate plate, but rather a splinter of the Africa plate, which is breaking up incoherently as it approaches the zone of collision. We suggest therefore thatthe Sinai block is not a small separate plate, and it is probably useless to try to find its western boundary.

(5) Finally, the zone of future seismic hazard associated with the Dead Sea fault has been outlined, as shown in Figure 38.

In summary, we have clarified the tectonics of a complex region, with relatively low seismic activity. Our study provides an unusual bridge between the features of local structural geology and elements of plate tectonics. This was done by focusing our effort on area of about 4° x 4° and crustal depth. To obtain good resolution on this scale it was best to use surface waves in the period range of 7 - 50 seconds.

Acknowledgements

We are indebted to Zvi Garfunkel for guiding us to the trace of the active strike slip near Jericho. We wish to thank Mr. Eli Arieh of the Geological Survey of Israel for supplying us with the Jerusalem and Ksara bulletins, Mr. Avi Shapira of the Weizmann Institute for useful comments, and Mr. Ezra Aboodi for helping us with the machine computations and initial motion diagrams. Dr. K. M. Goudarzi of the Institute of Geophysics, Tehran University, kindly sent us his publications. Technical assistance furnished by Miss Sara Fliegelman, Mr. Jehuda Barbut, Miss Tami Deutch and Ms. Kathleen Hart is highly appreciated. Finally, we convey our deep appreciation to Profs. Markus Bath (Uppsala), Erik Møller (Copenhagen), Ferdinand Steinhauser (Wien), M.J. Van Gils (Uccle), A.R. Ritsema (De Bilt) and the director of the Capetown station for kindly sending us their seismograms of the earthquake of July 11, 1927.

This research has been sponsored by the Cambridge Laboratories (AFCRL), United States Air-Force under Grant No. AFOSR-73-2528A at the Weizmann Institute of Science, and partially supported by Earth Science Section, National Science Foundation, Grants DES 75-04291 and DES-75-04874 at Stanford University.

REFERENCES

Abdel-Gawad, M., 1969. New evidence of transcurrent movements in Red Sea area and petroleum implications. The Am. Assoc. Petr. Geol. Bull. 55, 1466-1479.

Akasheh, B., 1972. Thickness of the crust in Iran. Bull. Fac. of Sci., Tehran Univ. 4, 63-69.

Akasheh, B. and S. Nasseri, 1972a. Die machtigkeit der Erdkruste in Iran. J. Earth Space Phys., Fac. of Sci., Tehran Univ. 1, 1-5.

Aki, K. and Y.B. Tsai, 1972. Mechanism of Love-wave excitation by explosive sources. J. Geophys. Res. 77, 1452-1475.

Aki, K., Reasenberg, P., DeFazio, T. and Y.B. Tsai, 1969. Near-field and far-field seismic evidence for triggering of an earthquake by the Benham explosion. Bull. Seism. Soc. Am. 59, 2197-2207.

Ambraseys, N.N., 1962. Data for the investigation of the seismic sea-waves in the eastern Mediterranean. Bull. Seism. Soc. Am. 52, 895-913.

Amiran, D., 1951. A revised earthquake Catalogue of Palestine. Israel Exploration J. 1, 223-246.

Amiran, D. (Ed.), 1970. Atlas of Israel. Survey of Israel. Ministry of Labor, Jerusalem and Elsevier Publ. Co., Amsterdam.

Arieh, E.J., 1967. Seismicity of Israel and adjacent areas. Geol. Survey of Israel Bull. 43, 1-14.

Ben-Menahem, A., 1975. Source parameters of the Siberian explosion of June 30, 1908 from analysis and synthesis of seismic signals at four stations. Phys. Earth. Plan. Int. 11, 1-35.

Ben-Menahem, A. and E. Aboodi, 1971. Tectonic patterns in the northern Red Sea region. J. Geophys. Res. 76, 2674-2689.

Ben-Menahem, A. and S.J. Singh, 1972. Computation of models of elastic dislocations in the earth. in: "Methods in Computational Physics,", v. 12, Bruce Bolt (ed.), Academic Press.

Blankenhorn, M., 1927, Das Erdbeben in Juli 1927 in Palastina. Zeitschr. Deutsch Palast. Ver. 50, 288-296.

Braslavski, Y., 1938. The earthquake and the stoppage of the Jordan river in 1546 (Hebrew). Zion, New Ser. 3, 223-336.

Brawer, A. J., 1928. Earthquakes in Palestine from July 1927, to August 1928 (Hebrew). Jew. Pal. Expl. Soc., 316-325.

Braile, L.W., R.B. Smith, G.R. Keller and R.M. Welch, 1974. Crustal structure across the Wasatch front from detailed seismic refraction studies, J. Geophys. Res. 79, 2669-2677.

Brune, J.J. and C.R. Allen, 1967. A low-stress drop, low-magnitude earthquake with surface faulting: the Imperial, California, earthquake of March 4, 1966. Bull. Seism. Soc. Am. 57, 501-514.

Buck, S.W., F. Press, D. Shepard, M.N. Toksoz, and H. Trantham, Jr., 1971. Development of a mercury tiltmeter for seismic recording. Rep. CSDL R-65, pp. 1-56. Dept. Earth Planet. Sci. Mars. Inst. of Tech., Cambridge, Mass.

Bulletin of the International Seismological Centre (ISC), Edinburgh 1968-1971.

Canitez, N. and S.B. Ucer, 1967. Computer determinations for the fault-plane solutions in and near Anatolia, Tectonop. 4, 235-244.

Canitez, N. and M. N. Toksoz, 19 . Static and dynamic study of earthquake source mechanism: San Fernando earthquake. J. Geophys. Res. 77, 2583-2594.

Chinnery, M.A., 1969. Earthquake magnitude and source parameters. Bull. Seism. Soc. Am. 59, 1969-1982.

De Vaux, R., 1961. L'Archeologie et les manuscrits de la mer morte. London.

Drake, C.L. and R.W. Girdler, 1964. A geophysical study of the Red Sea. Geophys. J.R. astr. soc. 8, 473-495.

Dubertret, L., 1932. Les formes structurales de la Syrie et de la Palestine, leur origine, C.R. Acad. Sci. Paris, 195, 66-68.

Freund, R., 1965. A model of the structural development of Israel and adjacent areas since upper Cretaceous times. Geol. Mag. 102, 189-205.

Fruend, R., 1970. The geometry of faulting in the Galilee. Israel J. Earth Sci. 19, 117-140.

Freund, R., Z. Garfunkel, I. Zak, M. Goldberg, T. Weissbrod, and B. Derin, 1970. The shear along the Dead Sea rift. Phil. Trans. Roy. Soc. Long. A 267, 107=130.

Gergawi, A. and H.M.A. El Khashab, 1968. Seismicity of Egypt. Helwan Obs. Bull. 76,

Girdler, R. W., 1965. The role of translational and rotational movements in the formation of the Red Sea and the Gulf of Aden in the world rift system, p. 65-95.

Girdler, R. W., 1958. The relationship of the Red Sea to the East Africa rift system, Quart. J. Geol. Soc. London, 114. 79-115.

Goudarzi, K.M., R. Soltanian and N. Mozafari, 1970. Etude de la croute terrestre a Shiraz. Bull. Fac. of Sci., Tehran Univ. 2, 34-41.

Gutenberg, B., 1955. Magnitude determination for larger Kern county shocks, 1952: Effects of station azimuth and calculation methods. in: Part II: Bulletin 171, Div. of Mines, Dept. Natural Resources, San Francisco.

Housley, R.M., B.R. Tittmann and E.H. Cirlin, 1974. Crustal Porosity information from internal friction profile, Bull. Seis. Soc. Am., 64, 2003-2004.

Ilan, Z., 1972. The Dead Sea and its shores (Hebrew). Tel-Aviv.

Josephus, . Antiquities of the Jews IX, 14.

Karnik, V., 1969, 1971. Seismicity of the European Area. Reidel Publ. Co., Dordrecht, Holland, Parts I-II.

Keller, W., 1955. The Bible as history.

Kenyon, N.H., A.H. Stride, and R.H. Belderson, 1975. Plan views of active faults and other features on the lower Nile cones. Inst. of Oceanographic Sci., Wormley, Godelming Survey, England (in press).

Le Pichon, X., J. Francheteau, and J. Bonnin, 1973. Plate Tectonics. Elsevier Sci. Publ. Co.

McKenzie, D.P., 1970. Plate tectonics of the Mediterranean region. Nature 226, 239-248.

McKenzie, D.P., 1972. Active tectonics of the Mediterranean region. Geophys. J.R. astr. Soc. 30, 109-185.

McKenzie, D.P. and W.J. Morgan, 1969. Evolution of triple junctions. Nature 224, 125-133.

McKenzie, D.P., and D. Davies, 1970. Plate tectonics of the Red Sea and east Africa. Nature, 226, 243-248.

Mitchell, B.J., 1973. Surface wave attenuation and crust anelasticity in Central North America, Bull. Seis. Soc. Am., 63, 1057-1072.

Neev, D., 1975. Tectonic evolution of the Middle East and the Levantine basin, Geology, 3, 683-687.

Neev, D. and K.O. Emery, 1967. The Dead Sea. Bull. No. 41, Ministry of Development Geological Survey, Jerusalem.

Niazi, M., 1968. Crustal thickness in the central Saudi Arabian peninsula. Geophys. J.R. astr. Soc. 15, 545-547.

Nowroozi, A.A., 1971, Seismo-tectonics of the Persian plateau, Eastern Turkey, Caucasus, and Hindu-Kush regions. Bull. Seism. Soc. Am. 61, 317-341.

Nowroozi, A.A., 1972, Focal mechanism of earthquakes in Persia, Turkey, west Pakistan, and Afghanistan and plate tectonics of the middle east. Bull. Seism. Soc. Am. 62, 823-850.

Nur, Amos, 1969. The effect of saturation on velocity in low porosity rocks, Earth & Plan. Sci. Lett., 7, 183-193.

Papazachos, B.C., 1973. Distribution of seismic foci in the Mediterranean and surrounding area and its tectonic implications. Geophys. J.R. astr. soc. 33, 421-430.

Papazachos, B.C., P.E. Comninakis, and J.C. Drakopoulos, 1966. Preliminary results of an investigation of crustal structure in southeastern Europe. Bull. Seism. Soc. Am. 56, 1241-1268.

Payo, G., 1967, 1969. Crustal structure of the Mediterranean sea by surface waves. Part I: Group velocity, Bull. Seism. Soc. Am. 57, 151-172 (1967); Part II: Phase velocity and travel times, Bull. Seism. Soc. Am. 59, 23-42 (1969).

Picard, L., 1966. Thoughts on the grabens system of the Near East. Geol. Survey Ppr. Can. 66-14, p. 22-34.

Plassard, J. and B. Kogoj, 1962. Catalogue des seisms ressentis au Liban. Annales-memoires de'l observatoire de Ksara, pp. 12.

Plassard, J. and B. Kogoj, 1973. Annales seismologiques de l'observatoire de Ksara 1961-1972.

Pomeroy, P.W., G. Hade, J. Savino, and R. Chander, 1969. Preliminary results from high-gain wide-band long-period electromagnetic seismographs systems. J. Geophys. Res. 74, 3295-3298.

Powell, M.J.D., 1970. "A hybrid method for non-linear equations" (pp. 87-114) and "A Fortran subroutine for solving systems of non-linear algebraic equations" (pp. 115-161). in: "Numerical Methods for Non-Linear Algebraic Equations", P. Rabinowitz (Ed.), Gordon and Breach Sci. Publ.

Quennell, A.M., 1959. Tectonics of the Dead Sea rift, Cong. Geol. Intern. Mexico, 1956. Session 20, Assoc. Serv. Geol. Africanos, 385-405.

Schaffner, H.J., 1959. Die grundlogen und auswerteverfahren zur seismischen bestimmung von erdbebenmechanismen. Akad.-Kerlor Berlin 1959 Frieberger Furschungshefte, C. 63.

Shalem, N., 1956. Tsunamis in the eastern Mediterranean (Hebrew). Bull. Israel Expl. Soc. 20, 159-170.

Shepard, D., 1971. Dynamic analysis of a mercury tiltmeter. Rep. CSDL E-2598, pp. 1-29, Mass. Inst. of Tech., Cambridge, Mass.

Shirokova, F.I., 1967. General features in the orientation of principal stresses in earthquakes foci in the Mediterranean-Asian seismic belt. USSR Earth Phys. Bull. Phys. Bull. Acad. Ser. 1, 22-36.

Sieberg, A., 1932. Untersuchungen uber erdbeben und bruchschollenbau im ostlichen mittelmeergebiet Jena, Verlag von Gustar Fischer.

Sieberg, A. 1932a. Erdbebengeographie. Hanbuch der Geophysik Band IV, Berlin, Verlag von Gebruder Borntraeger.

Spencer, J.W. and Amos Nur, 1975. Ultrasonic velocities in rocks under crustal conditions, J. Geophys. Res., in press.

Striem, H.L. and T. Milch. 1975. Tsunamis induced by sumbarine slumpings off Israel's coast (in press).

Takemoto, S., 1970. Strain steps and the dislocation fault model. Bull. Disaster Prevention Rase Inst. Kyoto Univ. 20, 1-15.

Tristram, H.B., 1865. The Land of Israel. London.

Tsai, Y.B. and K. Aki, 1969. Simultaneous determination of the seismic moment and attenuation of seismic surface waves. Bull. Seism. Soc. Am. 59, 275-287.

Tsai, Y.B. and K. Aki, 1970. Source mechanism of the Truckee, California earthquake of September 12, 1966. Bull. Seism. Soc. Am. 60, 1199-1208.

Vered, M. and A. Ben-Menahem, 1974. Application of synthetic seismograms to the study of low-magnitude earthquakes and crustal structure in the northern Red Sea region. Bull. Seism. Soc. Am. 64, 1221-1237.

Vered, M., A. Ben-Menahem and E. Aboodi, 1975. Computer generated P and S waves from an earthquake source in Iran. Pure and Appl. Geoph. 1,

Vilnai, Z., 1968. Judea and Samaria (Hebrew). Tel-Aviv.

Watson, C.Bm., 1975. The stoppage of the river Jordan in A.D. 1267. Quart. Stat. Pal. Expl. Fund. 253-261.

White, J.E., 1965. Seismic Waves, p. 102, McGraw Hill Book Co., NY, 302 p.

Wickens, A.J. and J.H. Hodgson, 1967. Computer re-evaluation of earthquake mechanism solutions 1922-1962. Publ. Domin. Obs. Ottawa.

Willis, B., 1928. Earthquakes in the Holy Land. Bull. Seism. Soc. Am. 18, 73-103.

Wu, F.T., I. Karcz, E.J. Arieh, U. Kafri, and U. Peled, 1973. Microearthquakes along the Dead Sea rift. Geology 1, 159-161.

Wyss, M. and J.N. Brune, 1968. Seismic moment, stress, and source dimensions for earthquakes in the California-Nevada region. J. Geophys. Res. 73, 4681-4694.

Yaari, A., 1943. Letters from the Land of Israel. "Gazit" Publ. House. Tel-Aviv.

Zak, I. and R. Freund, 1966. Recent strike-slip movements along the Dead Sea rift. Israel J. Earth Sci. 15, 13-37.

TABLE 1 : Zagros Mts. earthquake sources used for crustal structure studies

No.	Date	Origin time UT	P_n arrival at Eilat UT	Epicenter		M_B	h km	Distance to Eilat km	Azimuth to Eilat deg.	Inv. Azim. to Eilat deg.
				Lat.	Long.					
1	July 11, 1971	20 12 54.8	20 13 02	37.2°N	36.8°E	5.2	25	853	192	11
2	July 15, 1971	06 15 31.4	06 17 27	37.2°N	36.8°E	4.6	33	853	192	11
3	Aug. 17, 1971	04 29 33.1	04 31 22	37.1°N	36.8°E	5.0	33	842	192	11
4	June 29, 1971	11 13 42.3	11 15 41	37.3°N	36.9°E	4.6	31	866	193	12
5	July 1, 1971	23 15 07.1	23 16 59	37.2°N	36.9°E	4.5	33	855	193	12
6	June 12, 1972	13 34 00.7	13 36 23	33.1°N	46.3°E	5.4	33	1144	254	68
7	June 13, 1972	00 55 37.3	00 58 00	33.1°N	46.3°E	5.1	27	1144	254	68
8	June 14, 1972	04 34 28.1	04 36 51	33.0°N	46.1°E	5.3	33	1123	254	68
9	June 23, 1972	08 39 35.8	08 42 05	32.9°N	46.2°E	4.6	40	1129	254	69
10	June 10, 1972	19 31 41.8	19 34 06	32.9°N	46.3°E	4.0	33	1138	255	69
11	Jan. 14, 1972	22 10 03.7	22 12 35	32.8°N	46.9°E	5.1	33	1190	256	70
12	Sep. 27, 1973	02 27 21.4	02 29 04	32.7°N	48.4°E	4.2	41	1324	259	72
13	Sep. 30, 1973	21 00 22.5	21 03 04	32.6°N	48.3°E	4.3	50	1313	259	72
14	Nov. 22, 1974	09 04 46.1	09 07 49	32.7°N	49.8°E	4.1	58	1454	261	73
15	Nov. 22, 1974	09 44 17.0	09 47 21	32.7°N	50.0°E	4.6	52	1472	261	73
16	Mar. 12, 1973	13 21 49.1	13 24 43	32.1°N	49.3°E	4.9	62	1397	263	75
17	Mar. 13, 1973	06 03 49.0	06 06 45	32.1°N	49.4°E	4.9	33	1407	263	75
18	Mar. 12, 1974	01 45 35.9	01 48 44	32.2°N	50.2°E	4.4	34	1483	263	75
19	Mar. 14, 1973	03 45 41.7	03 48 39	32.0°N	49.4°E	4.5	33	1405	263	76
20	Aug. 6, 1973	05 31 45.0	05 34 47	31.1°N	49.9°E	4.5	48	1445	268	80
21	Aug. 5, 1973	09 44 52.3	09 47 56	31.1°N	50.0°E	4.6	33	1454	268	80
22	Oct. 17, 1974	04 10 15.8	04 13 12	30.9°N	49.6°E	4.6	35	1415	268	81
23	Aug. 15, 1973	04 35 42.9	04 38 46	30.9°N	50.0°E	4.1	33	1453	268	81
24	Apr. 5, 1973	19 24 01.6	19 27 10	30.9°N	50.5°E	4.0	33	1501	269	81
25	Apr. 22, 1973	21 29 57.2	21 32 54	30.7°N	49.8°E	5.0	57	1434	269	82
26	Sep. 22, 1971	12 24 22.8	12 27 30	30.5°N	50.3°E	4.8	33	1482	270	83
27	Aug. 2, 1974	08 23 44.0	08 26 51	30.5°N	50.6°E	4.8	44	1510	270	83
28	Jan. 6, 1972	09 41 33.2	09 44 41	30.3°N	50.5°E	5.2	41	1501	271	83
29	Dec. 15, 1971	15 24 57.4	15 28 04	30.2°N	50.6°E	4.9	42	1511	272	84

TABLE 2 : Earthquakes used for tectonics and crustal structure studies of the Afro-Eurasian junction

Id. No.	Date	Origin time UT	iP_n arrival at Eilat UT	Epicenter		Location	M	h(1) km	Distance, km				Azimuth, deg.				Inv. Azim., deg.			
				Lat.	Long.				EIL	JER	KSA	HLW	EIL	JER	KSA	HLW	EIL	JER	KSA	HLW
45*	July 11, 1927	13 04 07		32.0° N	35.5° E	N. of Jericho	6.2	5-7	264	36	206	463	192	268	10	240	11	47	190	58
47	Jan. 30, 1951	23 07 19		32.0° N	32.9° E	Off coast of Tel-Aviv	5.7	N	325	221	345	280	142	96	53	212	323	277	235	32
43	Apr. 8, 1951	21 38 08		36.5° N	35.7° E	Off coast of Iskanderun	5.7	N	761	525	297	841	185	185	177	210	5	5	357	28
44	Sep. 12, 1955	06 09 22		32.2° N	29.6° E	Off coast of Alexandria	6.1	N	583	533	615	308	117	94	71	147	300	276	255	328
30*	Mar. 26, 1968	19 37 34		34.1° N	35.5° E	Off coast of Beirut	4.8	15	494	258	47	613	186	186	130	221	6	6	310	39
31	Jan. 2, 1969	09 09 50	iP_IP 09 10 09	30.6° N	35.3° E	S. of the Dead Sea	3.0	-	109	131	362	390	198	357	9	259	18	177	189	77
46*	Mar. 31, 1969	07 15 54	07 16 26	27.7° N	34.0° E	Northern Red Sea	6.7	10-20	237	468	703	353	23	14	14	313	203	195	195	132
32*	Oct. 5, 1970	14 53 11	14 54 46	35.12°N	38.9° E	N.E. of Palmyra	4.7	32	710	504	311	919	213	224	243	233	31	42	62	49
33	Oct. 7, 1970	16 39 31	16 40 02.5	31.45°N	35.49°E	Dead Sea	3.5	-	204	45	266	435	195	325	8	247	15	145	188	65
34*	Oct. 8, 1970	02 45 41	02 46 12.5	31.45°N	35.49°E	Dead Sea	4.6	11-15	204	45	266	435	195	325	8	247	15	145	188	65
35	Dec. 19, 1970	22 44 09	22 44 45.5	27.5° N	33.9° E	Northern Red Sea	4.6	23	261	491	727	362	23	15	15	317	203	195	196	136
36*	Apr. 16, 1971	21 27 40	21 28 44	33.8° N	35.2° E	Off coast of Beirut	4.7	15	459	224	64	569	183	180	87	221	3	360	268	39
1*	July 11, 1971	20 12 56	20 14 49	37.2° N	36.8° E	Amanus-Taurus Mts.	5.1	25	853	618	383	959	192	194	193	213	11	13	12	30
37	Sep. 7, 1971	16 23 09	16 24 01	32.9° N	35.5° E	Upper Galilee	3.6	-	362	127	109	520	188	192	19	231	8	12	200	48
38*	Nov. 8, 1971	17 55 08	17 56 05	33.3° N	35.5° E	Southern Lebanon	4.0	2.5	406	170	69	549	188	189	32	227	7	9	212	45
39	June 28, 1972	09 49 35	09 50 12	27.6° N	33.8° E	Northern Red Sea	5.5	15	245	473	708	339	27	17	16	315	208	197	197	134
40*	Sep. 2, 1973	04 01 28	04 02 18.5	32.8° N	35.6° E	Sea of Galilee	4.3	7-9	353	118	117	520	190	198	13	232	10	17	193	50
41*	Apr. 29, 1974	20 04 40	20 05 25.5	30.5° N	31.7° E	Delta of the Nile	4.7	20	327	365	541	79	106	66	46	206	287	248	228	26
42*	June 12, 1974	10 19 51	10 21 03	34.0° N	37.7° E	S.W. of Palmyra	4.3	14	546	338	168	756	209	224	264	234	28	43	83	51

* Studies by spectral analysis

(1) Redetermined in present study from surface-wave spectra

Table 4: Results of Inversion of the Dispersion Data

Modified Niazi

H,km	α, km/sec	β km/sec	ρ $\frac{gm}{cm^3}$	σ
2.5	3.50	2.06	2.30	.235
12.0	5.70	3.40	2.55	.224
20.0	6.20	3.60	2.80	.246
60.0	8.10	4.60	3.40	.262
∞	8.70	4.90	3.65	.268

Eilat East

		R	L		σ
2.65	3.36	2.08	2.01	2.30	0.189
12.0	5.64	3.21	3.22	2.55	0.260
20.0	6.11	3.72	3.78	2.80	0.205
60.0	8.11	4.53	4.50	3.40	0.273
∞	8.70	4.90	4.93	3.65	0.268

Eilat North

				σ
2.6	3.42	2.08	2.30	.206
12.0	5.68	3.36	2.55	.231
20.0	6.10	3.78	2.80	.188
60.0	8.11	4.49	3.40	.279
∞	8.70	4.90	3.65	.268

Eilat-Amanus Mts.

				σ
2.5	3.45	2.08	2.30	.214
12.0	5.70	3.44	2.55	.214
20.0	6.10	3.81	2.80	.180
60.0	8.11	4.47	3.40	.282
∞	8.70	4.90	3.65	.268

TABLE 5: Summary of derived source elements of Near-East earthquakes

Date	azimuth, NφE, deg.			Slip[3] deg.	Dip deg.	Average $U_0 dS$ cm×km²	b km	v km/sec
	Strike	Dip	trend of motion					
Mar. 31, 1969[2]	330	45-60	5	315	45	45,000	30	3
July 11, 1927	10	100	9	350	85	18,000	45	2.2
Sep. 12, 1955[1]	315	45	331	332	57	-	-	-
Jan. 30, 1951[1]	159	249	350	331	70	-	-	-
Apr. 8, 1951[1]	305	35	348	125	50	-	-	-
July 11, 1971	270	0	0	90	27	215	<5	-
Mar. 26, 1968	200	290	30	333	70	45	-	-
Apr. 29, 1974	310	47	343	330	65	40	-	-
Apr. 16, 1971	171	261	12	318	64	38[4]	-	-
Oct. 5, 1970	60	150	40	39	64	30	-	-
Oct. 8, 1970	10	100	9	350	85	25	-	-
Sep. 2, 1973	10	100	9	350	85	10	-	-
June 12, 1974	60	150	42	39	67	10	-	-
Nov. 8, 1971	10	100	9	350	85	3	-	-

(1) Initial motions only (Canitez and Ücer, 1967).

(2) Ben-Menahem and Aboodi, 1971.

(3) Slip (λ) always indicates motion of hanging wall. Dip (δ) is that of footwall.

(4) Averaged over: AAE-R (40); EIL-R (35); EIL-L (40); HLW-R (25, possibly due to oceanic wave-path): MSH-L (38); NIL-L (40); TAB-L (40); POO-R (35); QUE-R (38); SHI-L,R (40).